LANDWARD MOISTURE FLUXES FOR THE NORTHERN HEMISPHERE

by

ARIBILOLA SAMUEL OMOLAYO

B.Sc., University of Ife, Nigeria (1974)
P.G. Dipl. Meteor., University of Ibadan, Nigeria (1976)

SUBMITTED IN PARTIAL FULFILLMENT OF THE

REQUIREMENTS FOR THE DEGREE OF

MASTER OF SCIENCE

at the

MASSACHUSETTS INSTITUTE OF TECHNOLOGY

August, 1980

Signature of Author. Signature redacted .....
Department of Meteorology and Physical Oceanography
August, 1980

Certified by... Signature redacted .....
Thesis Supervisor

Accepted by.... Signature redacted .....
Chairman, Department Committee on Graduate Students

LANDWARD MOISTURE FLUXES FOR THE NORTHERN HEMISPHERE

by

Aribilola Samuel Omolayo

Submitted to the Department of Meteorology and Physical Oceanography on August 8, 1980, in partial fulfillment of the requirements for the degree of Master of Science.

ABSTRACT

To obtain a better understanding of the hydrology of the Northern Hemisphere, the component of the total vertically integrated water vapor flux normal to all the coasts in the hemisphere has been computed from 5 years of homogeneous upper-air data. Values of this "landward" flux component together with those across the internal borders separating the various continents are used to compute the seasonal rates at which precipitation exceeds evapotranspiration over each continent. Maps of these normal fluxes and graphs containing values of them integrated over 10° latitude belts are presented. The maps simulate very well the low-level pattern of the general circulation of the atmosphere, while the graphs depict a range of interactions between land and ocean.

For the land masses of the Northern Hemisphere as a whole, the data show a moisture surplus exists in all seasons. While this also holds true for northern North America, it is not the case for many of the individual continents studied. The importance of monsoonal winds in the hydrological balance of the Northern Hemisphere is also evident. This study should prove useful to climate modeling efforts by serving both as a basis for comparison with model results and in making possible better parameterizations of the exchange of moisture between land and ocean.

Thesis Supervisor: Dr. Richard D. Rosen
Title: Visiting Lecturer

TABLE OF CONTENTS

ABSTRACT 2

TABLE OF CONTENTS 3

CHAPTER 1: INTRODUCTION 4

CHAPTER 2: THE BASIC EQUATIONS 10

CHAPTER 3: DATA AND PROCEDURES 14

CHAPTER 4: RESULTS 18

4.1 Fields of Landward Moisture Fluxes 18

4.1.1 Landward Moisture Fluxes for Winter 19
4.1.2 Landward Moisture Fluxes for Spring 21
4.1.3 Landward Moisture Fluxes for Summer 21
4.1.4 Landward Moisture Fluxes for Autumn 22
4.1.5 Summary 23

4.2 Landward Plus Internal Border Fluxes 24

4.3 Water Vapor Balance by Continent 25

4.4 Latitudinal Distribution of Landward Fluxes 30

CHAPTER 5: CONCLUSIONS AND SUGGESTIONS FOR FURTHER RESEARCH 34

APPENDIX 36

ACKNOWLEDGEMENTS 38

REFERENCES 39

LIST OF FIGURES 42

LIST OF TABLES 67

1. INTRODUCTION

An excess of evaporation over precipitation observed in some areas of the Earth and of precipitation over evaporation in some other areas attest to the great mobility of atmospheric moisture. The oceans represent a constant source of water from which the atmosphere over the continents replenishes its moisture, in addition to that supplied by evapotranspiration. The amount of water vapor in the atmosphere varies widely, both in space and in time, from a minimum of almost zero to values on the order of 0.6 percent of the total mass of an air column. Precipitaion processes and the large transport of water in the vapor phase by atmospheric circulations on various scales in space and time limit the average residence time of atmospheric water vapor to a little over a week. In short, there is a continual exchange of water vapor between the lands and the oceans across the coasts. The primary concern of this study is to compute this cross-coastal flow for the continents of the Northern Hemisphere using the most recent set of aerological data.

Hydrologists have approached water balance studies by applying the equation of continuity to water in its liquid state. This approach, which seeks the balance of precipitation, evapotranspiration, runoff, subsurface flow and the change in surface plus subsurface storage, is beset by many uncertainties. Even now the quality and non-stationarity of observational data do not allow accurate evaluation of some of the terms in the continuity equation. For example, evaporation processes are not yet fully understood

because of the non-uniformity of the evaporating surfaces; also, observed surface precipitation data involve non-random errors and tends to be underestimated (Anderson, 1964; LaRue and Younkin, 1963). In the first half of this century, in order to circumvent most of these problems and hence successfully quantify the water balance over a land surface, efforts were geared towards relating some of these quantities through empirical equations. Observed meteorological elements at the surface, observed evaporation from standard pans and porous water-filled globes, and moisture release from weighed boxes of earth were empirically related to total regional evapotranspiration by various investigators. Unfortunately, the noise in the data usually obscured the results.

An alternative approach to water balance studies is to consider the atmospheric branch of the hydrologic cycle by applying the principle of mass conservation for water in the atmosphere. This approach became feasible when the network of upper-air stations rapidly expanded over the globe in recent years. More sophisticated observing instruments also have come into use. Consequently there has been a large improvement in the quality and quantity of conventional aerological data now available. The objective of this aerological approach, therefore, is to study the large-scale atmospheric phase of the hydrologic cycle and to apply the findings resulting from such studies to evaluate the water balance at the Earth's surface.

Previous investigations of atmospheric water vapor can be broadly classified into two categories: regional and hemispheric. On a regional

basis, pioneering work was done by Benton, Blackburn and Snead (1950) and by Benton and Estoque (1954). They studied the water vapor content over North America for the year 1950. Folow-up work on North America was that of Rasmusson (1967). Using twice daily observations for the period May 1, 1961 to April 30, 1963, he found diurnal variations in the computed total vertically integrated moisture fluxes, particularly in summer. He attributed these variations to fluctuations in the mean wind rather than in the moisture. Similar studies have been made for some other regions. For instance, Peixoto and Obasi (1965) studied the humidity conditions over Africa during the IGY, while the seasonal variation of precipitable water vapor over India was studied by Anathakrishnan et al. (1965). Hutchings (1957) carried out similar studies for southern England for the summer of 1954 and four years later for the Australian continent (Hutchings, 1961). All of these regional studies utilized data collected over a period of at most two years. As summarized by Rasmusson (1975), these regional studies have led to a lower bound of about 2.5×10^5 square kilometers for the size of the region for which the equation of continuity of atmospheric water vapor gives reasonably useful hydrological results.

On the hemispheric scale, Starr and Peixoto (1958) measured the horizontal divergence of the vertically integrated flux over the Northern Hemisphere for the year 1950. Although the data used were sparse, they found centers of strong divergence over the Gulf of Mexico, the mid-Pacific, the Sahara, and southwestern United States. Furthermore, their work showed that centers of convergence are associated with the headwaters of many large rivers. A unique contribution of this work to hydrometeorology

was that it made available for the first time, on a hemispheric scale, water vapor flux divergence calculations based upon the atmospheric, rather than the surface, branch of the hydrologic cycle. Using these flux data, Lufkin (1959) presented a more detailed analysis of the hemispheric divergence field, and he found an empirical relation connecting the divergence of moisture flux over the oceans with oceanic salinity. Bannon and Steele (1960) published charts of atmospheric water vapor content for three standard isobaric surfaces--850, 700 and 500 mb--for the whole globe. Further hemispheric water vapor studies were made by Peixoto and Crisi (1965) for the IGY period, while Starr et al. (1969) presented pole-to-pole moisture conditions for the same year. Similarly, Oort and Rasmusson (1971) calculated and tabulated various atmospheric statistics for the Northern Hemisphere from 5 years of data. These statistics included seasonal and annual values of zonally averaged specific humidity, and the northward zonal mean transports of water vapor by transient and stationary eddies. A very recent attempt at studying moisture conditions over the Southern Hemisphere was undertaken by Viswanadham et al. (1980), who, despite the present sparseness of data for that region, presented the fields of mean precipitable water content for the four seasons of the year.

Most of the previous investigations of the fields of atmospheric water vapor have utilized data taken at a limited number of pressure surfaces and for a period of only one or two years. However, all of the data used for the present study have a better vertical resolution and cover a more extended period of 5 years, namely the period May 1, 1958 to April 30, 1963. With this high degree of data quality and the fact

that this same period has been widely studied by many previous investigators, such as Oort and Rasmusson (1971) and more recently by Peixoto, Salstein and Rosen (1980), I am confident that the results of the landward moisture flux computations which are presented in this thesis will be much more accurate than hitherto would be the case.

Apart from topography, another basic forcing of the general circulations of the atmosphere is the diabatic heating by latent heat release. The role of water vapor in the energetics of the general circulation of the atmosphere has been studied and discussed by Starr and White (1955), Starr and Peixoto (1965) and by Lorenz (1967) through the concept of available potential energy. Water vapor has also been recognised as the most important factor in radiative processes in the atmosphere, regulating the energy balance through the absorption and transmission of radiation (Sutcliffe, 1956).

Because of the fundamental importance of water vapor to the atmosphere, general circulation and long-range forecasting models have attempted to parameterize evaporative heat loss from the surface of the Earth and the heat gained by the atmosphere because of latent heat release. These attempts have not been entirely successful, however, despite their sophistication (Manabe, Smagorinsky and Stricker, 1965; Holloway and Manabe, 1971). These general circulation models (GCM) tried to incorporate the atmospheric phase of the hydrologic cycle through the three-dimensional advection of water vapor, moist convective adjustment, evaporation from the earth's surface, condensation and precipitation. There are, also, the more simple two-dimensional global climate models like those constructed by Sellers (1973) and Robock (1977) which utilize an idealized land-water

distribution. In addition, in these climate models many of the inputs are specified. Yet, in spite of the approximations and idealizations, these two classes of models do simulate some of the basic features of the general circulation. The computations of cross-coastal flow presented here, therefore, will enable more realistic parameterizations to be used in the Seller-type models and will also serve as a basis against which the GCM's can be compared. Finally it is hoped that the present work will form another useful contribution toward understanding more completely the hydrology of the Northern Hemisphere.

2. THE BASIC EQUATIONS

As previously mentioned, the hydrometeorological approach to water balance studies seeks to apply the principles of mass conservation to water in the atmosphere. This approach is as follows. Assuming the atmosphere to be in a state of hydrostatic equilibrium, then the co-ordinate system (λ, ϕ, p, t) where λ represents longitude, ϕ the latitude, p, t pressure and time respectively, is appropriate for this kind of study. If we consider an atmospheric column above a given point on the earth's surface to be of sufficient vertical extent such that there is a negligible water mass at the top, the mean zonal component, $\overline{Q}_\lambda$, and the mean meridional component, $\overline{Q}_\phi$, of the vertically integrated moisture flux, as well as the mean precipitable water $\overline{W}$ are respectively given by

$$\overline{Q}_\lambda = \frac{1}{g}\int_{p_T}^{p_o} \overline{qu}\,dp \qquad (1a)$$

$$\overline{Q}_\phi = \frac{1}{g}\int_{p_T}^{p_o} \overline{qv}\,dp \qquad (1b)$$

$$\overline{W} = \frac{1}{g}\int_{p_T}^{p_o} \overline{q}\,dp \qquad (1c)$$

where u, v are the eastward and northward components of the wind at a given pressure surface, q the corresponding specific humidity, p_o, p_T the pressure at the ground surface and at the top of the chosen column, while g is the acceleration due to gravity. The overbar represents a time average, which can be defined for a time interval τ for any quantity as

$$\overline{(\;)} = \frac{1}{\tau}\int_{\tau}(\;)\,dt$$

In this study, τ represents the length of a composite season, while p_T equals 300 mb.

Taking precipitation and evaporation processes in the atmosphere into consideration, the general balance equation for the water content in the atmosphere is usually expressed (Peixoto, 1973)

$$\frac{\partial W}{\partial t} + \nabla \cdot \underset{\sim}{Q} = E - P \qquad (2)$$

where $\underset{\sim}{Q}$ is the two-dimensional vector representing zonal, Q_λ, and meridional, Q_ϕ, transports of water vapor. P is the precipitation out of the column and E is the evapotranspiration into the base of the column.

For hydrological purposes we now consider integrating (2) over an area A bounded by a contour l, with the outward pointing unit normal vector $\underset{\sim}{n}_o$ at any point on this boundary. Using the Ostrogradsky-Gauss theorem, integrating equation (2) yields

$$\frac{1}{A}\int \frac{\partial W}{\partial t} dA + \frac{1}{A}\oint (\underset{\sim}{Q}\cdot\underset{\sim}{n}_o) dl = \frac{1}{A}\int (E-P) dA$$

Taking the time average of this equation and using angle brackets to denote the area average of a quantity, we have:

$$\left\langle \overline{\frac{\partial W}{\partial t}} \right\rangle + \frac{1}{A}\oint \overline{\underset{\sim}{Q}\cdot\underset{\sim}{n}_o}\, dl = \left\langle \overline{E-P} \right\rangle \qquad (3)$$

For long-term studies (seasonal or annual) the rate of change of water vapor stored in the atmosphere is generally much smaller in magnitude than the remaining terms. If in addition, then, we assume that the flux

divergence and storage changes of the condensed phase are negligible, then the excess (or deficit) of evapotranspiration over precipitation over a given area for a unit time interval can be reliably given by the total flux per unit time crossing the boundary; that is

$$\frac{1}{A}\oint \overline{\underset{\sim}{Q}\cdot\underset{\sim}{n}_o}\,dl = \langle\overline{E-P}\rangle \qquad (4)$$

Hydrologists are more interested in net landward transports than in ocean-ward transports. For this reason, equation (4) can be re-expressed to become

$$\frac{1}{A}\oint \overline{\underset{\sim}{Q}\cdot\underset{\sim}{n}_i}\,dl = -\langle\overline{E-P}\rangle = \langle\overline{P-E}\rangle \qquad (5)$$

with $\underset{\sim}{n}_i$ becoming an inward (landward) pointing unit normal vector at any point on the coast. Defining a scalar quantity Q_p equal to $\overline{\underset{\sim}{Q}\cdot\underset{\sim}{n}_i}$ and then choosing a constant distance interval Δl of coastline, a step-wise integration of equation (5) gives

$$\frac{1}{A}\sum Q_p \Delta l = \frac{\Delta l}{A}\sum Q_p = \langle\overline{P-E}\rangle \qquad (6)$$

Q_p, therefore, is the value of $\overline{\underset{\sim}{Q}\cdot\underset{\sim}{n}_i}$ evaluated at the midpoint of each distance interval Δl. It is normal to Δl and points inwards towards the land (see Appendix).

We also have

$$Q_p = \bar{Q}_\lambda \cos\gamma + \bar{Q}_\phi \sin\gamma \qquad (7)$$

where γ represents the angle which $\underset{\sim}{n}_i$ makes with the local eastward direction at that particular midpoint, and it is approximated by the geometric expressions

$$\tan\gamma \cong \frac{\lambda_a - \lambda_b}{\phi_a - \phi_b}\cos\tfrac{1}{2}(\phi_a + \phi_b) \qquad (8)$$

In this expression, ϕ_a , λ_a are respectively the latitude and the longitude at the beginning of the interval while ϕ_b , λ_b are those at its end. The beginning and the end of an interval are determined so that land is to the left as you go from the beginning of the interval to the end; that is, so the normal points inwards. The derivation for ν is found in the appendix. Finally, therefore, we have

$$\frac{\Delta l}{A} \sum \left(\overline{Q}_\lambda \cos\nu + \overline{Q}_\phi \sin\nu \right) = \langle \overline{P-E} \rangle \qquad (9)$$

Based on the definition of Q_p, equation (9) implies that, for a given portion of land during a given season, if the summation on the left-hand side turns out to be positive, then there is an excess of precipitation over evapotranspiration; but if the sign is negative, then that area is dominated by evapotranspiration.

3. DATA AND PROCEDURES

The basic meteorological data used are the specific humidity, q, and the eastward and northward wind components u and v. The original data were daily radiosonde observations taken at approximately 550 stations at 00 GMT during the 60 month period, May 1958 through April 1963. These data form part of the MIT General Circulation Library (Starr et al., 1970). The locations of the stations are displayed in Figure 1. The data were available at every 50 mb from the surface to 300 mb and have been previously widely studied by Oort and Rassmusson (1971) and more recently by Peixoto, Salstein and Rosen (1980). The data were divided into four composite seasons such that winter, for instance, is defined as the ensemble of 15 December, January and February months.

All of the data were entered into an objective analysis scheme that generated two-dimensional analyses of the vertical integrals of moisture fluxes at grid points on a polar-stereographic map of the Northern Hemisphere. These analyses, along with the streamfunction derived from them, are presented by Peixoto et al. (1980) and are repeated here in Figures 2-13. Large versions of these maps, as well as the background grid, were available for use in this study.

A preliminary step in this investigation was to construct a polar stereographic map of the coastline of the various continents in the

Northern Hemisphere using a distance interval of 300 nautical miles (about 555 kilometers). This distance appeared reasonable in the light of the resolution of the available data. The map construction was made so that the essential features of the coastlines were very well reproduced (Fig 14). It is worth noting that part of the coastlines of South America and Africa extend slightly into the Southern Hemisphere because it is not realistic to divide the coasts north of the equator into an exact number of equi-distant intervals.

Certain small scale features do not appear in Figure 14 because of the resolution used. For example, the Suez disappears, thereby linking the Mediterranean Sea with the Red Sea. As a result, Africa has a continuous coastline from the Indian Ocean on the east to the Atlantic on the west. Elsewhere, because the English Channel is such a narrow waterway, it becomes neglected in this reconstructed map. Hence the coast of France is linked directly with Iceland and Britain, thereby making these islands appear like a triangular strip jutting into the North Atlantic.

Figure 14 shows how the continents have been separated while Table 1 lists the number of coastline segments, the length of coast, and the area of each continent north of the equator. The areas were obtained by planimetry and they were found to be in agreement with atlases. To facilitate direct usage and to lend themselves to comparisons with previous investigations, separate computations are made for United States plus Canada, Mexico, and South plus Central America. Also for the purpose

of this study, the boundary between Europe and Asia is placed at longitude 42°E on the northern coastline while their southern boundary is put at longitude 36°E.

The net difference between precipitation and evapotranspiration over each of those regions marked in Figure 14 is of basic hydrological interest. This quantity has actually been given by equation (5), that is

$$-\frac{1}{A}\int \overline{\nabla\cdot\underset{\sim}{Q}}\,dA = \frac{1}{A}\oint \overline{\underset{\sim}{Q}\cdot\underset{\sim}{n}_i}\,dl = \langle\overline{P-E}\rangle$$

Expressing area in square meters, l in meters and Q_p in kilogram per second per meter, $\langle\overline{P-E}\rangle$ then has units of kilograms per squared meter per second. If we now divide this by the density of liquid water, it then turns out that

$$10\,kg\,m^{-2}s^{-1} = 1\,cm\,s^{-1}$$

Therefore a division of the left-hand-side of equation (5) by a factor of 10 gives the difference between precipitation and evapotranspiration for the particular region being considered in units of $cm\,s^{-1}$. This quantity can alternatively be expressed in centimeters per 3 months or per year. This thesis represents the first time that computations of $\langle\overline{P-E}\rangle$ have been made for all of the continents of the Northern Hemisphere using the same homogeneous set of simultaneous data. Also the results obtained here can be used to compare with earlier $\langle\overline{P-E}\rangle$ computations for those regions like North America or Africa that have been studied before.

For the purpose of computing $\langle \overleftarrow{P-E} \rangle$ for each of the regions in Table 1, the internal borders separating them have been marked off using the same 300 nautical mile distance interval used for the coasts. These borders are shown by dashed lines in the base map (Fig. 14). While the moisture fluxes (Q_p) across just the coasts of the Northern Hemisphere for each of the four composite seasons are presented in Figures 15-18, they are combined with those computed for the internal borders (shown in dashed arrows) in Figures 19-22.

4. RESULTS

4.1 Fields of Landward Moisture Fluxes.

The fields of the two-dimensional cross-coastal fluxes for the four composite seasons are presented in Figures 15-18. These maps agree well with the streamfunction analyses computed by Peixoto et al. (1980), which for completeness were displayed in Figures 10-13, except over the southern portion of India in summer. This difference may be attributed to the fact that only the non-divergent part of the wind is used to formulate those streamfunction analyses. Although the individual Q_p vectors have been drawn locally normal to the coast in Figures 15-18, the general direction of the arrows shows clearly the basic low-level wind patterns of the general circulation of the atmosphere over the Northern Hemisphere. Since almost all of the water vapor in the atmosphere is concentrated below the first two kilometers, it is not surprising that these maps reproduce very well the easterlies of the low and high latitudes, as well as the westerlies of subtropical and middle latitudes.

Both wind and humidity measurements go into computing moisture fluxes. However, when considering the component of the flux normal to the coast, the orientation of the coast is also an important factor. The alignment of the coast can either magnify or dampen the resulting fluxes. An instance of this effect is found in Figure 15: where a flux of 0.02 $kg\,s^{-1}m^{-1}$ can

be found in the Gulf of Mexico. The zonal and meridional components of the vertically integrated flux that went into yielding this small net landward flux are 80 and 61 $kg\,s^{-1}m^{-1}$ respectively. In this illustration, the part of the flux normal to the coast resulted from two fluxes of almost equal strength but opposite signs. Clearly, care must be taken when interpreting or using each of Figures 15-18.

4.1.1 Landward Moisture Fluxes for Winter.

The map for winter is presented in Figure 15. It is clear from the map that in the tropics, moisture is brought into the continents by easterly winds through three major paths. The most extensive of these stretches along the coasts of Central and South America up to the Gulf of Mexico. Because of the orientation of the coast, moisture crosses them almost zonally. In addition these winds are fairly strong during the winter months, leading to high landward fluxes for the region. On the other hand the weak fluxes within the Gulf of Mexico result from the orientation of its coast, as noted above.

The two other zones of entry within the easterlies are of much shorter length. These are along the east coast of Africa, including the Gulf of Aden in the Red Sea, and a rather diffuse zone covering the coast of Burma, the Gulf of Siam and the coast of Vietnam. The landward fluxes in both of these regions are rather intense. The reason for this is the presence of steady trade winds that blow from Asia over the Persian Gulf and into Africa almost at right angles to the coast within the Gulf of Aden. Though these

winds are rather dry, their strength more than compensates for their low moisture content. The trade winds that blow over the Gulf of Siam are of the same origin and characteristics as those described for Africa.

The westerlies blow over more latitude belts and over greater land areas than the easterlies. We have, therefore, rather widespread but consistently small landward fluxes along the west coast of the United States and Canada. These combine over the heart of the continent with those fluxes from the Gulf of Mexico (Benton and Estoque, 1954) to form a long stretch of oceanward fluxes along the east coast from Hudson Bay to Florida. In contrast the westerlies that enter Europe are very intense. This is probably due in part to the long ocean track of the winds from the east coast of North America, and also because the European coast is almost everywhere oriented perpendicular to the winds. Consequently, with very few exceptions, landward fluxes exist everywhere along the coast of Europe. Part of the westerly wind stream from North America enters Africa through its northwestern sector, passing over the Red Sea, the Persian Gulf and the Gulf of Oman into Asia. These westerlies exit Asia along its entire east coast with the exception of a small region in the northeast where polar easterlies bring in moisture. Generally speaking, in the region of the easterlies, we have positive (landward) moisture fluxes along the east coasts and negative fluxes across the west coasts of the various continents. The reverse picture holds for those coastal regions that come under the influence of the westerlies: positive fluxes on the west coasts and negative ones on the east coasts.

4.1.2 Landward Moisture Fluxes for Spring.

The map of the landward moisture fluxes for the months of spring is presented in Figure 16. A comparison of this map with that for winter reveals great similarity between the two. The basic moisture flux pattern during winter is also present in spring. Easterlies still form a continuous belt around the hemisphere, as do the westerlies. However, there are slight modifications from winter in some areas both with regard to the pattern and to the magnitude of the fluxes. Thus, in spring the fluxes are generally weaker than in winter. Also strong fluxes appear to occur farther north in spring. An example of changes from the winter pattern occurs in the Gulf of Mexico, where those fluxes that were almost non-existent in winter have suddenly intensified. On the other hand, Q_p values in Florida have been reduced by a factor of two. These modifications generally occur in the zones separating the tropical easterly fluxes from the subtropical westerly fluxes. The northward progression of the subtropical westerlies has been attributed (Peixoto et al., 1980) to the northward migration of the subtropical anticyclones.

4.1.3 Landward Moisture Fluxes in Summer.

Summer is the only season when the low latitude easterly flow is interrupted by south-westerly monsoonal winds over some portions of Africa, India and southeast Asia (Fig. 17). In those regions, therefore, the zone of tropical easterlies is greatly narrowed and pushed northwards as the subtropical highs weaken and move northward in summer. However, because monsoonal winds have long ocean tracks, they are laden with much moisture

as they cross into the Northern Hemisphere. Consequently strong landward fluxes are observed along the coasts in these regions. Except for this intrusion by the monsoons, the basic flux pattern described for winter even persists into Summer. However, stronger fluxes than for Winter and Spring combined are observed around the Gulf of Mexico. The reason for this is because the winds become more southerly in this region (Fig. 12), so that the meridional component of the vertically integrated transport, Q_ϕ, becomes much stronger than before. This fact is clearly illustrated by Figures 6-10 where it can be seen that the summer maximum of 128 $kgs^{-1}m^{-1}$ for Q_ϕ is about 50% higher than Q_ϕ for Winter.

Generally speaking, land-ocean contrasts in the zone of the mid-latitude and subtropical westerlies are much more marked in Summer than in any other season. This is, of course, as expected, since much more water is evaporated in Summer because of the high insolation.

4.1.4 Landward Moisture Fluxes for Autumn.

The map of the fluxes for autumn is presented in Figure 18. The distribution of the fluxes resembles closely that of Summer. However, the monsoonal winds have disappeared from Africa and Southeast Asia, but persist over India, even though they are much weakened. The overall picture is that fluxes are weaker in autumn than in summer. Very weak fluxes due to the polar easterlies are found northeast of USSR and over Japan.

4.1.5 Summary.

In the annual mean, therefore, the low-level general circulation pattern of easterlies and westerlies persist through all four seasons, except for the modification of the tropical easterlies in summer by the emergence of the monsoons of the Eastern hemisphere. This pattern as a whole generally shifts northwards in spring, reaches its farthest northern limit in summer and then begins a southward migration to complete an annual cycle. Consequently, in the zone of the easterlies, the east coasts of the continents become regions of landward moisture transports while moisture exits through the west coasts. The opposite picture holds for those latitude belts that come under the influence of the westerlies. The cross-coastal fluxes are strongest for summer.

It is obvious from the maps that the west coast of the United States and Canada provides an entry for moisture, while the east coast of Asia acts as an exit all year round. Fluxes are consistently directed landwards along the coast of Europe. As for Africa, fluxes along the Mediterranean are of a diverse nature, but are landward in the annual mean.

4.2 Landward Plus Internal Border Fluxes.

Although the maps in Section 4.1 depict land-ocean contrasts, they do not contain all the information needed about the water balance for the specific regions shown in Figure 14. For this purpose, the fluxes across the internal borders are also needed. These are included in Figures 19-22. The combined transports across the coasts and across the internal borders are presented in Table II for each region. A division of these quantities by the areas of the continents or sub-continents yields the values for $\langle \overline{P-E} \rangle$ shown in Table III. Table IV gives just the cross-coastal transports.

A comparison of Tables II and IV reveals that fluxes across the internal borders can have a very significant impact on the total transport into a region. Naturally, where two regions share a common border, what amounts to a moisture loss for one region becomes a gain for the other. Europe and Asia in summer provide a good example of this. The cross-coastal summer value for Europe, from Table IV, is 0.949×10^{8} kg s^{-1}. With the addition of its internal border with Asia, however, the sign is completely reversed. The loss to Asia is so enormous that the summer transport for Asia goes up nearly an order of magnitude. Perhaps a more startling illustration is that of the United States plus Canada versus Mexico. These two regions have only 3 segments of internal border in common. In no season is the landward transport value in Table IV for Mexico negative, but the inclusion of the internal borders shows that much of the moisture going into Mexico is actually being transported over land into the United States. Mexico's net transport (Table II), therefore, is negative all of the seasons except for summer.

4.3 Water Vapor Balance by Continent.

The approach to be adopted in this section will be to discuss the more interesting or unusual results found in Table II, rather than to discuss all the seasonal transport values for each continent and subcontinent. At the outset, it is worth noting that moisture transports across the coasts of Greenland represent an insignificant contribution to either Europe or America. The weak fluxes computed for Greenland are due to the fact it lies largely within the weak and very variable polar easterlies. Consequently, Greenland will be omitted from further discussion in this section.

Comparing Tables II and IV, it is found that Africa north of the equator and Europe lose moisture across their internal borders all year except for Africa in summer, while America north of the equator gains moisture throughout the year (except for a slight loss in winter). The loss experienced by Europe is, of course, transported into Asia, while that by Africa is to the Southern Hemisphere across the equator. Similarly, the increase in the transport into America comes from across the equator. The net effect of these inter-hemispheric moisture fluxes on the convergence of moisture over the land masses of the Northern Hemisphere is, like for America, to decrease it in winter and to increase it for the other seasons. Interestingly, though, the net convergence over the land of the Northern Hemisphere still remains positive in winter, despite the fact that there is an overall loss of moisture by the entire Northern Hemisphere to the Southern Hemisphere that season.

According to Table IV, both America and Europe gain moisture from the oceans all year. However America's seasonal landward transport values are greater than the corresponding values for Europe, except in autumn. The reason for this is that America spans the belt of the westerlies and the moist tropical easterlies, in addition to its much longer coastal length. These, therefore, provide a better chance for America to derive more moisture, chiefly through the west coasts and the Gulf of Mexico.

The third zone of moisture flow into America north of the equator is, as noted before, through the equatorial border. The annual transport across the equator into America is about 0.64×10^{8} kg s^{-1}, with the greatest seasonal transport occurring in autumn. Why this cross-equatorial transport into America is largest in autumn has to do with the low-latitude easterlies in this region. To accomplish this transport, these easterlies must gain a southerly component in autumn, in contrast to the northerly component they have in winter that is responsible for the transport of moisture from America to the Southern Hemisphere in winter.

A region of great hydrological interest on the basis of my results is Mexico. With the Gulf as a moisture source to the east and an over-land moisture influx from Central America, it is surprising that only in summer does Mexico have a positive convergence (Table II). In the annual mean, too, Mexico exports more moisture than it receives. The line separating the easterlies from the westerlies passes over the northern fringe of Mexico, and this will, therefore, be a region of variable fluxes. Can this

introduce an error in the sampling of the data? Even if it does, can the error be so large as to reverse the signs of these transports? If the evapotranspiration actually exceeds precipitation in the annual mean, as indicated by Table III, it would seem worth studying what other fresh water sources are available to Mexico, noting that the Rio Grande is the only river of significance in the region and there is no large lake.

From Table IV, it is seen that ocean-to-land transports for Africa north of the equator are low. The surrounding oceans and seas constitute moisture sources for Africa in winter, spring and summer. However the large autumnal negative value more than balances the transports for the other 3 seasons, to the effect that the net annual landward value of -0.05×10^{8} kg s^{-1} for Africa represents a net flow from Africa to the ocean.

This picture for Africa is, however, much different when the transports across the equator are included (Table II). The net convergence is now generally one order of magnitude higher. Except for summer, large amounts of moisture are lost to the Southern Hemisphere every season. The value in Table II is fairly uniform from autumn through winter. However, a dramatic change occurs from winter to spring, when moisture begins to converge over north Africa. This convergence peaks in summer. The summer maximum results from the monsoons which blow over portions of Africa during this season. The influence of these winds, with their high moisture contents, is often felt as far north as latitude 22°N, corresponding, over West Africa, to the northward limit of the inter-tropical convergence zone (ITCZ).

As is apparent in Figure 18, fluxes along the coast of Africa are generally oceanward in autumn, except along the north-east sector. The corresponding oceanward transport when added to the smaller southward transport across the equator accounts for the large autumnal loss for Africa. The Hadley cell begins its southward journey in autumn. Consequently the central Atlantic anticyclone begins to weaken, and the westerlies spread southwards to bring more of the southern portion of Africa under their influence. On the other hand, the Saharan high intensifies at this time. The presence of this continental high inhibits the incursion of the westerlies into North Africa, so they are forced to assume a north-westerly direction over Africa. Therefore only very weak westerly fluxes enter North Africa, while the Mediterranean coastal region provides a moisture exit. Further south along the west coast, the easterlies still prevail and serve to carry moisture away from the land. Hence, like Mexico, Africa suffers an overall moisture deficit, amounting to about 0.3×10^{8} kg s^{-1} in the annual mean.

The coast of Asia is comparable in length to that of America. However, the entire east coast of Asia is a potential exit for moisture. Except for the incursion of the monsoons into southeast Asia and India in summer, large amounts of moisture are lost through that sector. It is not surprising, therefore, that Asia should record negative convergence values for all seasons except summer, in spite of the high seasonal inter-continental moisture transports from Europe into Asia. However, unlike for Mexico or Africa, this single high summer value enables Asia to record a net annual

positive convergence value. This happens to a large extent because of the contributions made by the Indian monsoon. Like the Asian continent as a whole, India is a source of moisture for the atmosphere above the oceans for all seasons except summer. The summer monsoon is so intense over India that the landward transport then is at least 4 times the ocean-ward transport at any other time over India. And the net annual transport of 0.03×10^{8} kg s^{-1} over India accounts for a sizeable portion of the net annual transport for the whole continent.

On the hemispheric scale, Table II shows the Northern Hemisphere has a moisture surplus all year, despite the negative landward value for autumn in Table IV. It is clear from Table IV that, essentially, it is the moisture loss across the coasts of Asia in autumn that accounts for the negative autumnal hemispheric value in that Table. Anyway, as noted above, the convergence of moisture into the whole hemisphere is still positive in autumn, even though it has the lowest magnitude among all the seasons. Clearly, it is the transport from the Southern Hemisphere into America that has made the difference.

The values of $\langle \overleftrightarrow{P-E} \rangle$ in units of cm(3 months)$^{-1}$ presented in Table III show America north of the equator to be the wettest continent, especially in its central and southern regions. Africa is the driest continent even though its $\langle \overleftrightarrow{P-E} \rangle$ value for summer is about twice that for Asia. The highest inter-continental moisture transport between Europe and Asia takes place in summer, and its effect has resulted in a precipitation deficit for Europe for this season. The values for the United States plus Canada shown in this Table tend to be larger than what Rasmusson (1966) obtained for this region, although both show summer to be the driest season. The difference can possibly be attributed

to the choice of different periods for both studies (it is known that inter-annual fluctuations in weather do occur; Rosen et al., 1979). Also Rasmusson utilized twice-daily data, while once-a-day data have been used in the present study. The hemispheric value of $\langle \overline{P-E} \rangle$ which is seen to be highest in summer demonstrates the importance of the monsoons in the overall hydrological balance of the Northern Hemisphere.

4.4 Latitudinal Distribution of Landward Fluxes.

While Table II gives the net convergence over each of the regions being studied, seasonal landward transports by 10° latitude belts are presented in Table V. It should be emphasized that transports across the equator do not enter into this Table.

By latitude bands, the annual mean picture from Table V is that of net landward (positive) fluxes in the tropics, with the maximum occuring in summer between latitudes 20°N and 30°N. In contrast, there is a loss of moisture to the oceans between 30°N and 50°N, followed by a gain from the oceans in somewhat higher latitudes. In the polar regions north of 70°N, the land again supplies moisture to the oceans. Seasonally, however, differences from this annual mean picture do exist.

A check of the 10°N-20°N latitude band shows the east coast of Central America and the region around the Gulf of Aden, in the Red Sea, to be the two principal regions contributing positively in this belt during the winter months. In summer, however, the former is the only dominant region of positive fluxes within the belt. The net large landward transport in

winter is because the easterlies are mostly zonal in those two regions (Figs. 2 and 6). The 20°N to 30°N latitude belt, on the other hand, comes under the partial influence of the westerlies in winter. The intensification of the Pacific and the central Atlantic highs in summer forces the southern edge of the westerlies northwards, thus allowing for deeper penetration of the monsoons. Although all continents constitute moisture sources for the oceans in winter between 20°N and 30°N, the greatest loss occurs in Africa along the Red Sea coast. In the annual mean, however, there is net landward transport in this belt. This is made possible by the transports along the American and Asian west coasts in summer. In particular, the contribution by Asia is about 4 times that of America, and about 50% of this Asian contribution is clearly attributable to the monsoons.

The next 20° of latitude, from 30°N-50°N, is characterized by negative fluxes during all seasons except winter. The greatest oceanward transport occurs in summer between 40°N and 50°N. In this belt, the Mediterranean coastal area represents a region of variable fluxes in the annual mean. This is chiefly due to the mountinous terrain of southern Europe and also to the rapid fluctuations in the orientation of the coast. Since the 30°N-50°N belt is characterized by westerlies, fluxes exit the continents along their east coasts. The general orientation of the fluxes is southward as is evident from Figures 15-18. Consequently the land in this latitude zone is also a moisture source region for the lower latitudes, in concert with moisture transports from the Southern Hemisphere. This, therefore, helps to account for the positive transport values recorded for the 20°N-30°N

latitude belt.

The presence of high terrain along the west coast of North America forces the winds to release their moisture as orographic precipitation before they penetrate very far inland. The influx from the Gulf of Mexico produces strong oceanward fluxes along the east coast of the United States. Since the influence of the fluxes from the Gulf of Mexico is not deeply felt as far north as latitude 50°N, only very weak fluxes are observed along the east coast of North America for the 50°N-70°N latitude belt. Unlike for America, though, the westerlies are not inhibited by any marked topography along the west coast of Europe. This allows for deeper penetration of moisture into Eurasia and accounts for the much stronger fluxes observed along European coasts. In the middle latitudes, much of the moisture transports within the westerlies is due to the baroclinic eddies. These eddies are usually seen on surface synoptic maps as closed cyclonic and anticyclonic systems, and as trough and ridge patterns at upper levels. In addition the 50°N-70°N belt has the longest coastal length. This more than compensates for the weak landward fluxes that characterize the northern portion of the zone.

North of latitude 70°N, the region is mostly water. The existing landmass is principally northern Greenland. Being the zone of the weak and highly variable polar easterlies, moisture is generally transported from the land to the oceans.

If precipitation exceeds evapotranspiration for a complete latitude band (land plus ocean), does the land supply the ocean with water in that belt or does the ocean supply the lands with water? To answer this important land-ocean water vapor contrast question, the graph of the zonally averaged divergence of water vapor, $[\nabla \cdot \underset{\sim}{Q}]$, as a function of latitude, was plotted for each season and for the year (Rosen, 1980, personal communication). These are presented in units of centimeters per second in Figure 23. Superimposed on each of these graphs is the plot of the landward transports of water vapor, $\int Q_p \, dl$, in units of kilograms per second; also as a function of latitude. Therefore, in the former plot,

$$[\nabla \cdot \underset{\sim}{Q}] = [E - P]$$

while in the latter, positive values imply a supply of moisture to the land by the oceans in the specified latitude belt.

From viewing where the $[\nabla \cdot \underset{\sim}{Q}]$ plot crosses the zero line in the annual mean composite graph, Table VI was derived. In this Table only the signs of the quantities rather than their magnitudes were considered. According to Table VI, no general answer can be provided to the question. In the equatorial region, as well as in the region north of 35°N, precipitation exceeds evapotranspiration for the latitude belts as a whole; a reverse picture is true for the sub-tropics. However, the cross-coastal transport is generally landward (positive) all the way up to latitude 35°N and alternates for the remainder of the hemisphere.

5. CONCLUSION

The present study has been concerned with computing the component of water vapor flux normal to the coasts of the continents in the Northern Hemisphere in an attempt to present a better understanding of land-ocean moisture contrasts. Maps of the computed fluxes simulate the seasonal low-level wind pattern of the general circulation, in support of the fact that the greatest part of the atmospheric branch of the hydrologic cycle actually lies within the lower portion of the atmosphere.

An attempt was made in section 4.4 to answer a pertinent question about land-ocean moisture contrasts. However, a more fundamental hydrological question still remains, namely, if precipitation exceeds evapotranspiration for a whole latitude belt (land plus ocean), does precipitation necessarily exceed evapotranspiration for the land or the ocean individually within that belt? This is an important topic for future research. I have shown that the quantity $\langle \overline{P-E} \rangle$ over several of the regions studied is highly sensitive to transports across the internal borders. Since the transports across these borders are shown in section 4.2 to be highly significant and strong meridionally, the meridional flux of water vapor into or out of a region should be considered and not neglected (Lufkin, 1959) in such a study.

Perhaps the single most important result in this study is the quantity $\langle \overline{P-E} \rangle$ which is computed simultaneously, for the first time, for all the

continents of the Northern Hemisphere and for the hemisphere as a whole. These values, presented in Table III, show, for example that Africa north of the equator is a region of moisture divergence. An explanation for how this deficit is balanced can possibly be found in the concept of subterranean water (Starr and Peixoto, 1958). On the other hand, I found that the land portion of the Northern Hemisphere enjoys a moisture surplus through the year.

Judging from the quality of the basic wind and humidity data that went into this study and the fact that the same data and period have been studied by previous investigators (Oort et al., 1971; Peixoto et al., 1980), I have confidence in the basic findings of this study. Any disagreement between these results and those of other investigators can be due to one or more of the reasons given in Section 4.3. It is, however, my expectation that climate modelers will find the results of this work useful as a basis for comparison with the results of their complex general circulation models and the results here will also afford a better parameterization of the basic processes modeled in the more simple approaches.

APPENDIX

1. Landward flux of moisture Q_p.

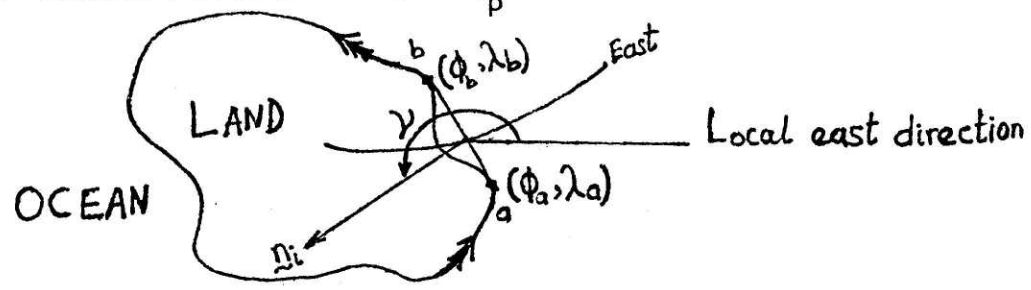

$$Q_p = \underset{\sim}{Q} \cdot \underset{\sim}{n}_i = Q_\lambda \cos\gamma + Q_\phi \cos\gamma$$

The double arrow indicates the direction of moving around the coast in the calculations. A negative value of Q_p implies that the land supplies moisture to the oceans at that portion of the coastline.

2. Angle Gamma (γ)

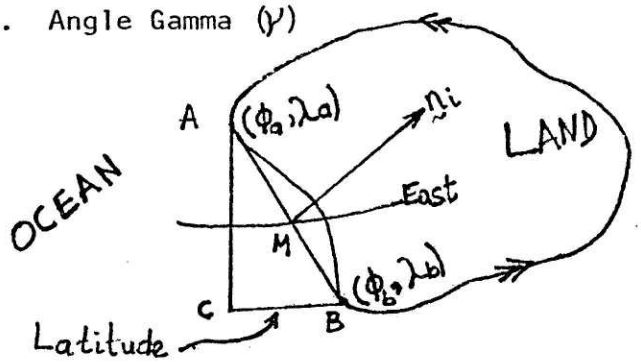

The angle γ is that angle which the inward pointing unit normal vector makes with the local eastward direction at any portion of the coastline; and it is derived here for the case in which it is acute. In deriving γ only longitude was taken to increase westwards.

AB is a unit length of the coast with midpoint M.

Using geometry, angle CAB is also γ .

Distance along longitude AC = $R(\phi_a - \phi_b)$

Distance along latitude CB = $R(\lambda_a - \lambda_b)\cos\phi_m$

R is the radius of the earth and ϕ_m is the latitude for the midpoint M. In the limit as A→B; $\phi_m \cong \frac{1}{2}(\phi_a + \phi_b)$ gives a reasonable weighting factor. Hence

The quandrant in which each angle γ lies is given by the following table

$\lambda_a - \lambda_b$	+	+	-	-
$\phi_a - \phi_b$	+	-	-	+
quadrant	I	II	III	IV

ACKNOWLEDGEMENTS

I am particularly grateful to Dr. Richard D. Rosen for supervising this work. His constant interest, guidance and encouragement all helped in making it a reality.

The helpful suggestions of Professor Reginald E. Newell are likewise appreciated.

Mrs. Kathy Huber skillfully typed the manuscript and Miss Isabelle Kole drafted the figures. Additional help was provided by Miss Susan Ary. My gratitude goes to them all.

As is usual, my wife, Oluwabunmi, was an asset to me during this effort. Her assistance and words of encouragement constantly renewed my strength and carried me through. I am deeply indebted to her.

The basic data were collected and analysed by Dr. Richard D. Rosen through the support of the Division of Atmospheric Sciences, National Science Foundation, under Grant ATM-7716348.

REFERENCES

Anathakrishnan, R., Selvan, M. M. and Chellappa, R., 1965: Seasonal variation of precipitable water vapor in the atmosphere over India. India J. Meteor. Geophys. 16, 371-384.

Anderson, T., 1964: Further studies on the accuracy of rain measurements. Arkiv fUr Geofysik 4, 16.

Bannon, J. K. and Steele, L. P., 1960: Average water vapor content of air. Met. Office, Geophysical Memoir No. 102, 38.

Benton, G. S., Blackburn, R. T. and Snead, V. O., 1950: The role of the atmosphere in the hydrologic cycle. Trans. AGU 31, 61-73.

Benton, G. S. and Estoque, M. A., 1954: Water vapor transfer over the North American continent. J. Meteor. 11, 462-477.

Holloway, J. L. and Manabe, S., 1971: Simulation of climate by a general circulation model. Mon. Weather Rev. 99, No. 5, 335 pp.

Hutchings, J. W., 1957: Water vapor flux and flux divergence over Southern England: Summer 1954. Quarterly Journal of Royal Met. Soc. 83, 30-48.

Hutchings, J. W., 1961: Water vapor transfer over the Australian continent. J. Meteor. 18, 615-634.

La Rue, J. A. and Younkin, R. T., 1963: Large scale precipitation volumes, gradients, and distribution. Mon. Weather Rev. 91, 393-401.

Lorenz, E. N., 1967: The nature and theory of the general circulation of the atmosphere. WMO, Geneva, 169 pp. (WMO-No. 218.TP115).

Lufkin, D., 1959: Atmospheric water vapor divergence and the water balance at the earth's surface. Sci. Rep. No. 4, General Circulation Project, MIT, 44pp.

Manabe, S., Smagorinsky, J. and Strickler, R. F., 1965: Physical climatology of a general circulation model with a hydrologic cycle. Mon. Weather Rev. 93, 769-798.

Oort, A. H. and E. M. Rasmusson, 1971: Atmospheric Circulations Statistics. NOAA Prof. Paper No. 5 (NTIS COM-72-50295), 323 pp.

Peixoto, J. P. and Crisi, A., 1965: Hemispheric humidity conditions during the IGY. Sci. Rep. No. 6, Planetary Circulations Project, MIT.

Peixoto, J. P. and Obasi, G. O. P., 1965: Humidity conditions over Africa during the IGY. Sci. Rep. No. 7, Planetary Circulations Project, MIT.

Peixoto, J. P., 1973: Atmospheric vapor flux computations for hydrologic purposes. WMO/IHD Report No. 20 (WMO-No 357).

Peixoto, J. P., Salstein, D. A. and Rosen, R. D., 1980: Intra-annual variation in large-scale moisture fields. Jour. Geophysical Research, in press.

Rasmusson, E. M., 1966: Atmospheric water vapor transport and the hydrology of North America. Report No. A-1, Planetary Circulations Project, MIT.

Rasmusson, E. M., 1967: Atmospheric water vapor transport and the water balance of North America. Mon. Weather Review 95, 403-425.

Rasmusson, E. M., 1975: Hydrologic application of atmospheric vapor flux analyses. Report of the WMO/CHY Rapporteur (unpublished).

Robock, A. D., 1977: Climate predictability and simulation with a global climate model. Ph.D. Thesis, Dept. of Meteorology, MIT.

Rosen, R. D., Salstein,D. A. and Peixoto, J. P., 1979: Variability in the annual fields of large-scale atmospheric water vapor transport. Mon. Weather Rev., 107, 26-37.

Sellers, W. D., 1973: A new global climatic model. Jour. Appl. Meteor. 12, 241-254.

Starr, V. P. and White, R. M., 1955: Direct measurement of the hemispheric poleward flux of water vapor. J. Marine Res. 14, 217 -225.

Starr, V. P. and Peixoto, J. P., 1958: On the global balance of water vapor and the hydrology of deserts. Tellus 10, 189-194.

Starr, V. P. and Peixoto, J. P., 1964: The hemispheric eddy flux of water vapor and its implications for the mechanics of the general circulation. Arch. Met. Geoph. Biokl. 14, 111-130.

Starr, V. P., Peixoto, J. P. and McKean, R., 1969: Pole-to-pole moisture conditions for the IGY. Pure and Appl. Geoph. 75, 300-331.

Starr, V. P., Peixoto, J. P. and Gaut, N. E., 1970: Momentum and zonal kinetic balance of the atmosphere from five years of data. Tellus 22, 251-274.

Sutcliffe, R. C., 1956: Water balance and the general circulation of the atmosphere. Quarterly Journal of Royal Met. Soc. 82, 385-395.

Viswanadham, Y., Rao, N. J. M. and Nunes, G. S. S., 1980: Some studies on moisture conditions in the Southern Hemisphere. Tellus 32, 131-142.

LIST OF FIGURES

Figure Number		Page
1	Distribution of aerological stations used in the investigation.	43
2	Hemispheric distribution of the vertically integrated zonal moisture transport, Q_λ, for composite winter season during 1 May 1958 - 30 April 1963 (from Peixoto et al., 1980). Units are 10 kg $s^{-1}m^{-1}$. Negative values indicate westward flow.	44
3	Same as in Figure 2 but for composite spring season.	45
4	Same as in Figure 2 but for composite summer season.	46
5	Same as in Figure 2 but for composite autumn season.	47
6	Hemispheric distribution of the vertically integrated meridional moisture transport, Q_ϕ, for composite winter season during 1 May 1958 - 30 April 1963 (from Peixoto et al., 1980). Units are 10 kg $s^{-1}m^{-1}$. Negative values indicate westward flow.	48
7	Same as in Figure 6 but for composite spring season.	49
8	Same as in Figure 6 but for composite summer season.	50
9	Same as in Figure 6 but for composite autumn season.	51
10	Hemispheric distribution of the streamfunction for the vertically integrated moisture transport, Ψ, for composite winter season during 1 May 1958 - 30 April 1963 (from Peixoto et al., 1980). Units are 10^7kg s^{-1} and arrows indicate the sense of circulation.	52
11	Same as in Figure 10 but for composite spring season.	53
12	Same as in Figure 10 but for composite summer season.	54
13	Same as in Figure 10 but for composite autumn season.	55
14	Base map of the continents as reconstructed for this study.	56
15	Landward moisture fluxes in winter. Units are in kg $s^{-1}m^{-1}$.	57
16	Same as in Figure 15 but for spring.	58
17	Same as in Figure 15 but for summer.	59
18	Same as in Figure 15 but for autumn.	60

Figure Number		Page
19	Landward moisture fluxes plus the fluxes across the internal borders in winter. Units are kg $s^{-1}m^{-1}$.	61
20	Same as in Figure 19 but for spring.	62
21	Same as in Figure 19 but for summer.	63
22	Same as in Figure 19 but for autumn.	64
23	Plot of the landward moisture transports as a function of latitude and the zonally averaged water vapor divergence for the complete latitude belt. Units for the former are 10^{8}kg s^{-1} and for the latter 10^{-6}cm s^{-1}.	65
24	Same as in Figure 23 but for complete year.	66

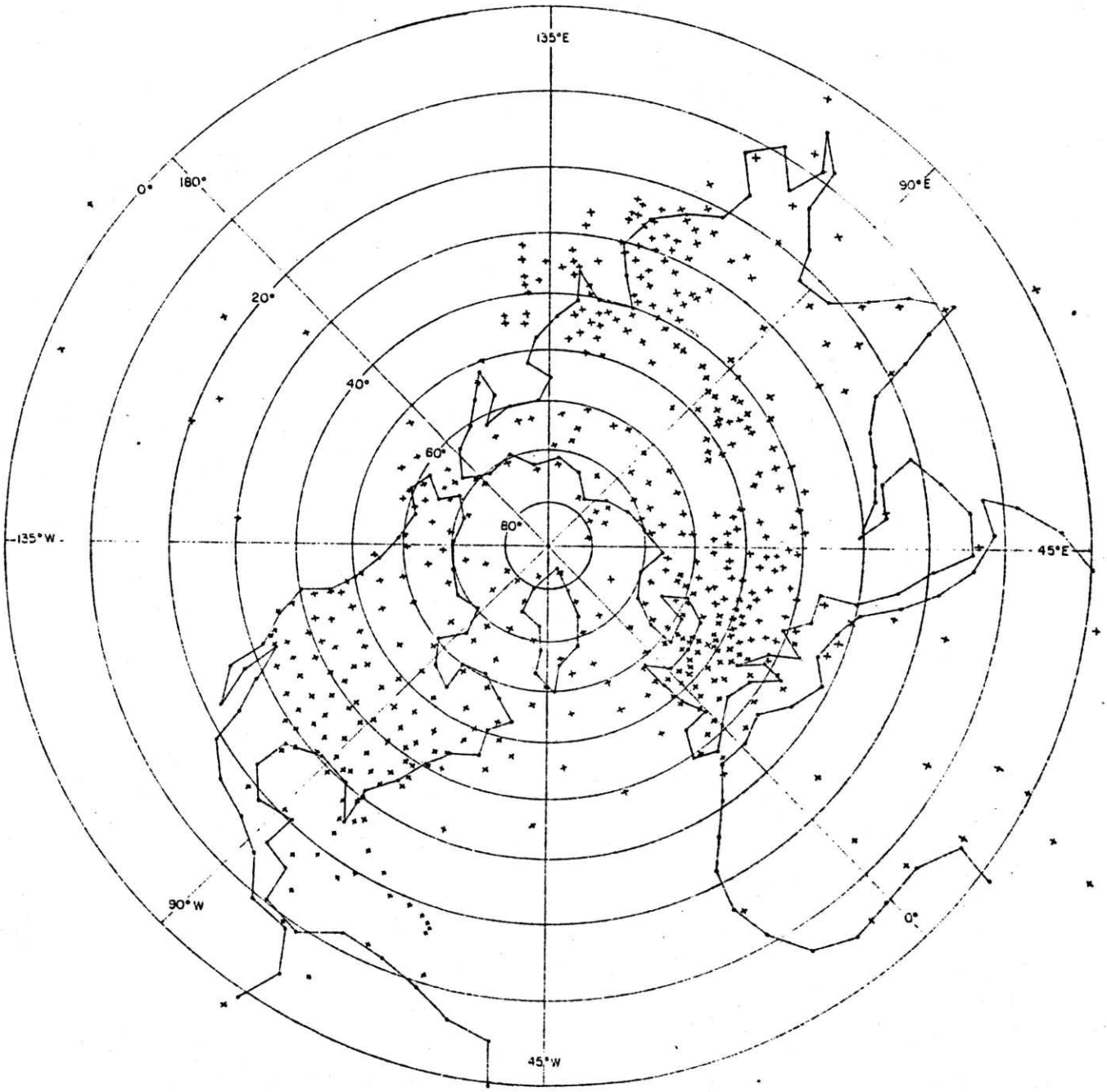

Figure 1. Distribution of aerological stations used in the investigation.

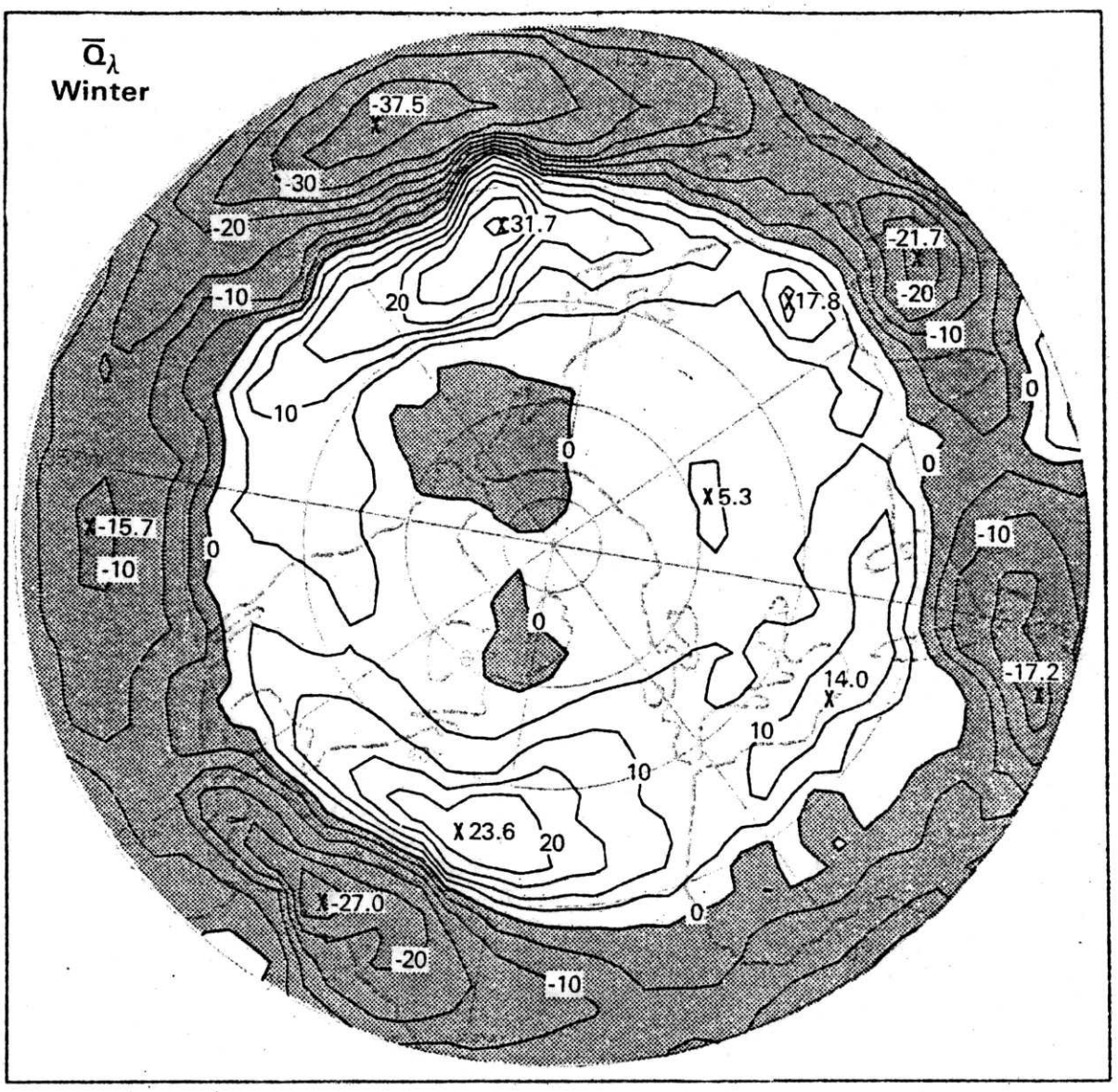

Figure 2. Hemispheric distribution of the vertically integrated zonal moisture transport, Q_λ, for composite winter season during 1 May 1958 - 30 April 1963 (from Peixoto et al., 1980). Units are 10 kg $s^{-1} m^{-1}$. Negative values indicate westward flow.

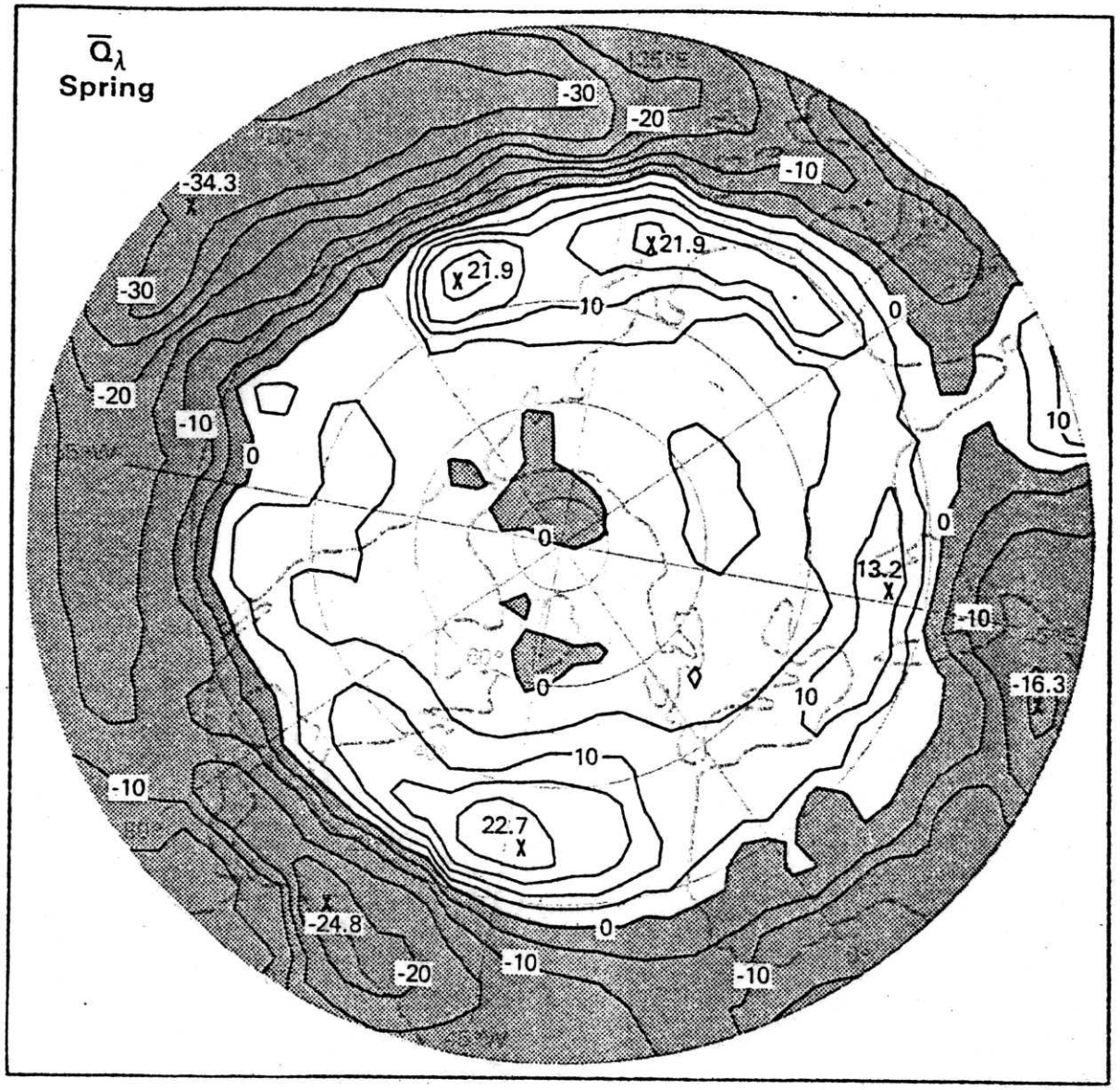

Figure 3. Hemispheric distribution of the vertically integrated zonal moisture transport, Q_λ, for composite spring season during 1 May 1958 - 30 April 1963 (from Peixoto et al., 1980). Units are 10 kg $s^{-1} m^{-1}$. Negative values indicate westward flow.

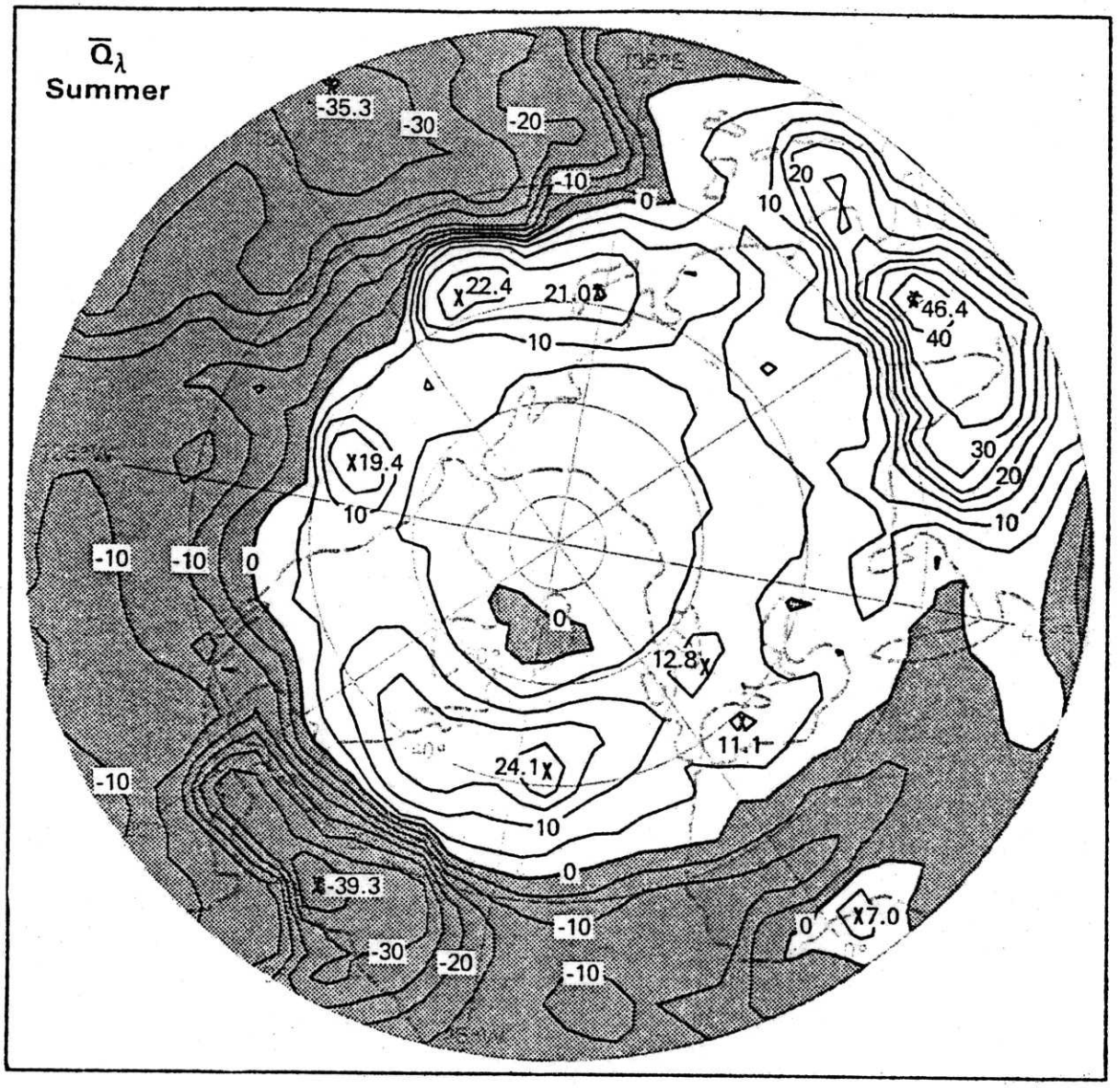

Figure 4. Hemispheric distribution of the vertically integrated zonal moisture transport, Q_λ, for composite summer season during 1 May 1958 - 30 April 1963 (from Peixoto et al., 1980). Units are 10 $kg\,s^{-1}m^{-1}$. Negative values indicate westward flow.

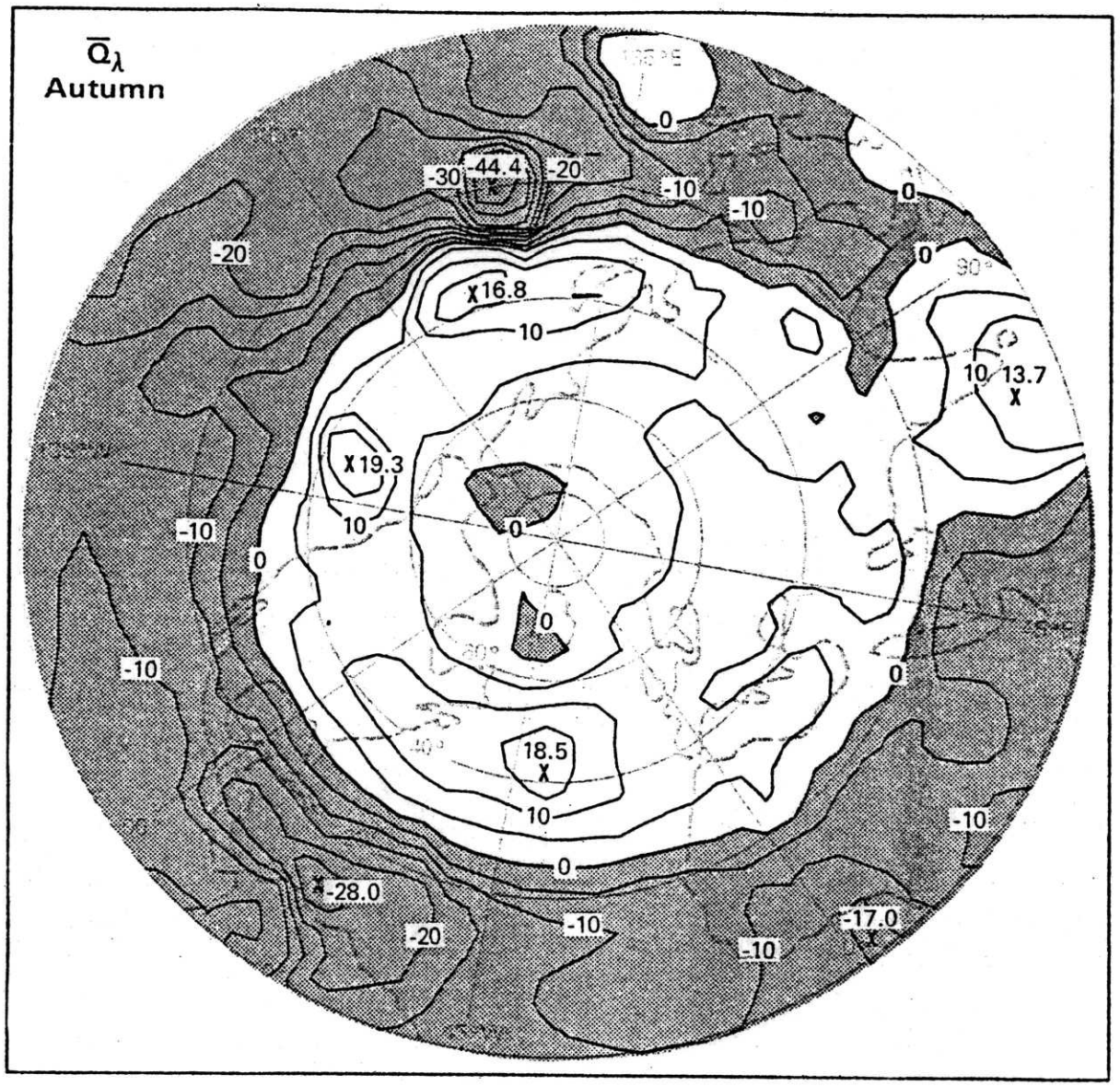

Figure 5. Hemispheric distribution of the vertically integrated zonal moisture transport, Q_λ, for composite autumn season during 1 May 1958 - 30 April 1963 (from Peixoto et al., 1980). Units are 10 kg $s^{-1}m^{-1}$. Negative values indicate westward flow.

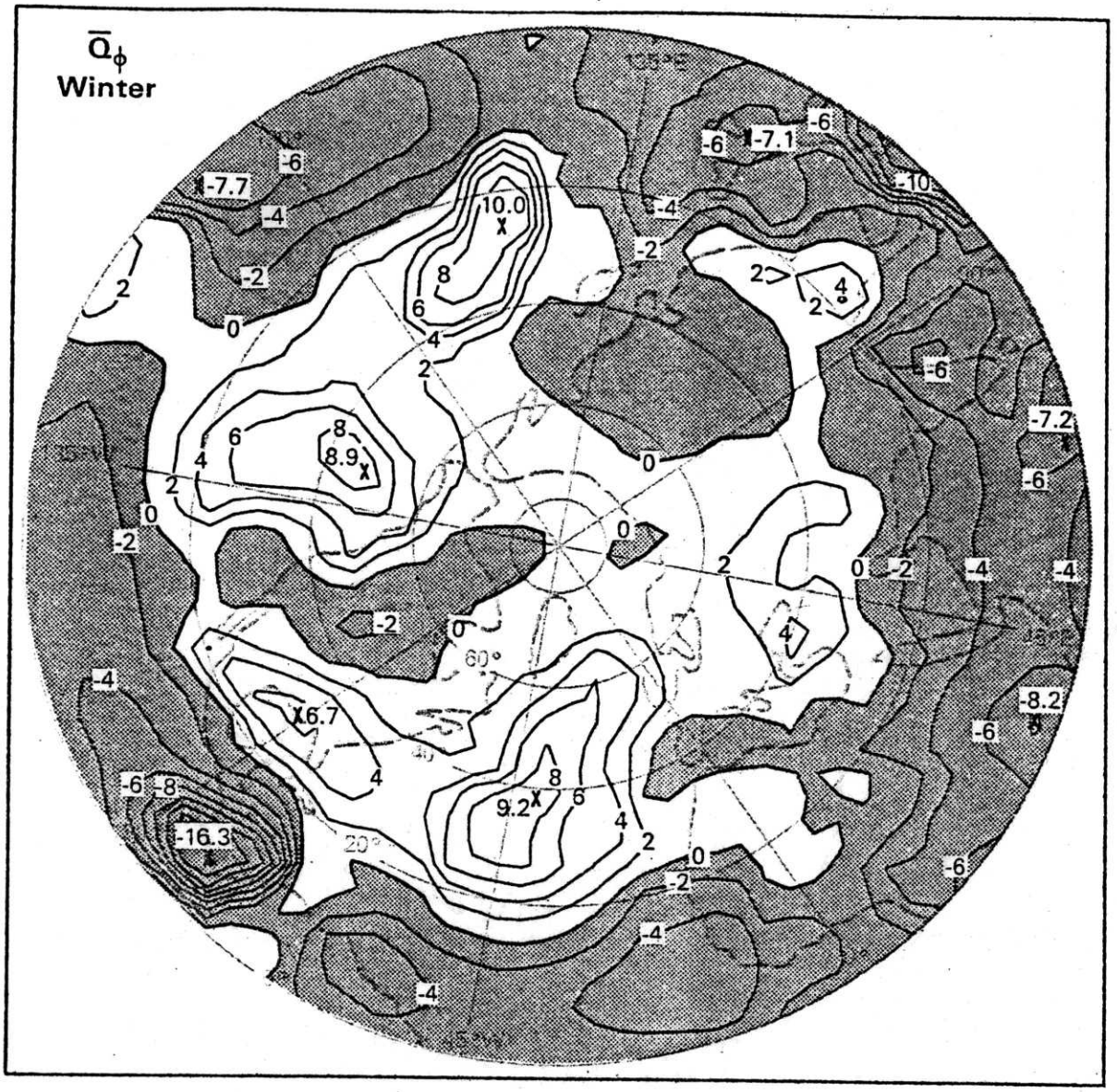

Figure 6. Hemispheric distribution of the vertically integrated meridional moisture transport, Q_ϕ, for composite winter season during 1 May 1958 - 30 April 1963 (from Peixoto et al., 1980). Units are 10 kg $s^{-1}m^{-1}$. Negative values indicate westward flow.

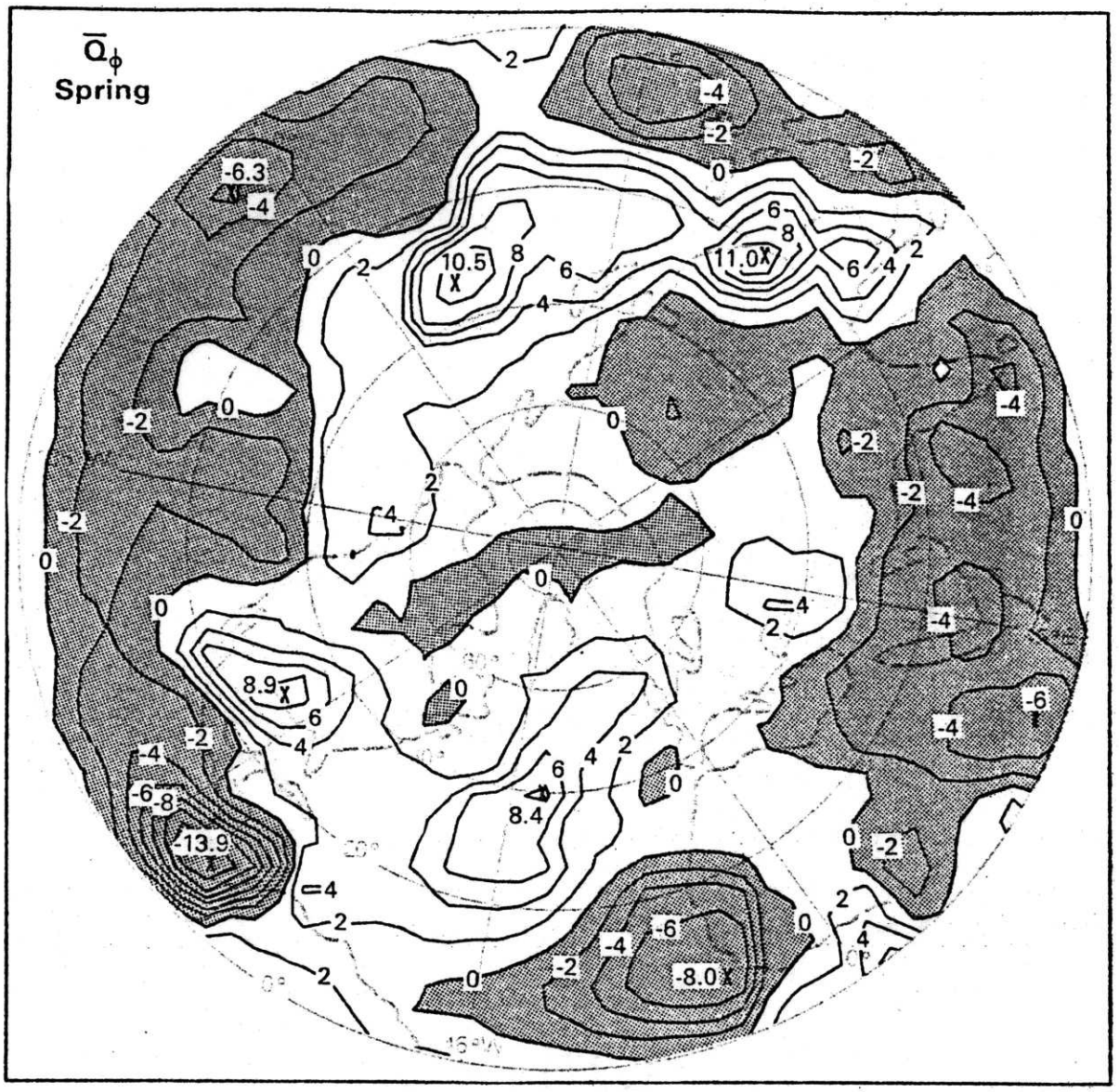

Figure 7. Hemispheric distribution of the vertically integrated meridional moisture transport, Q_ϕ, for composite spring season during 1 May 1958 - 30 April 1963 (from Peixoto et al., 1980). Units are 10 kg $s^{-1}m^{-1}$. Negative values indicate westward flow.

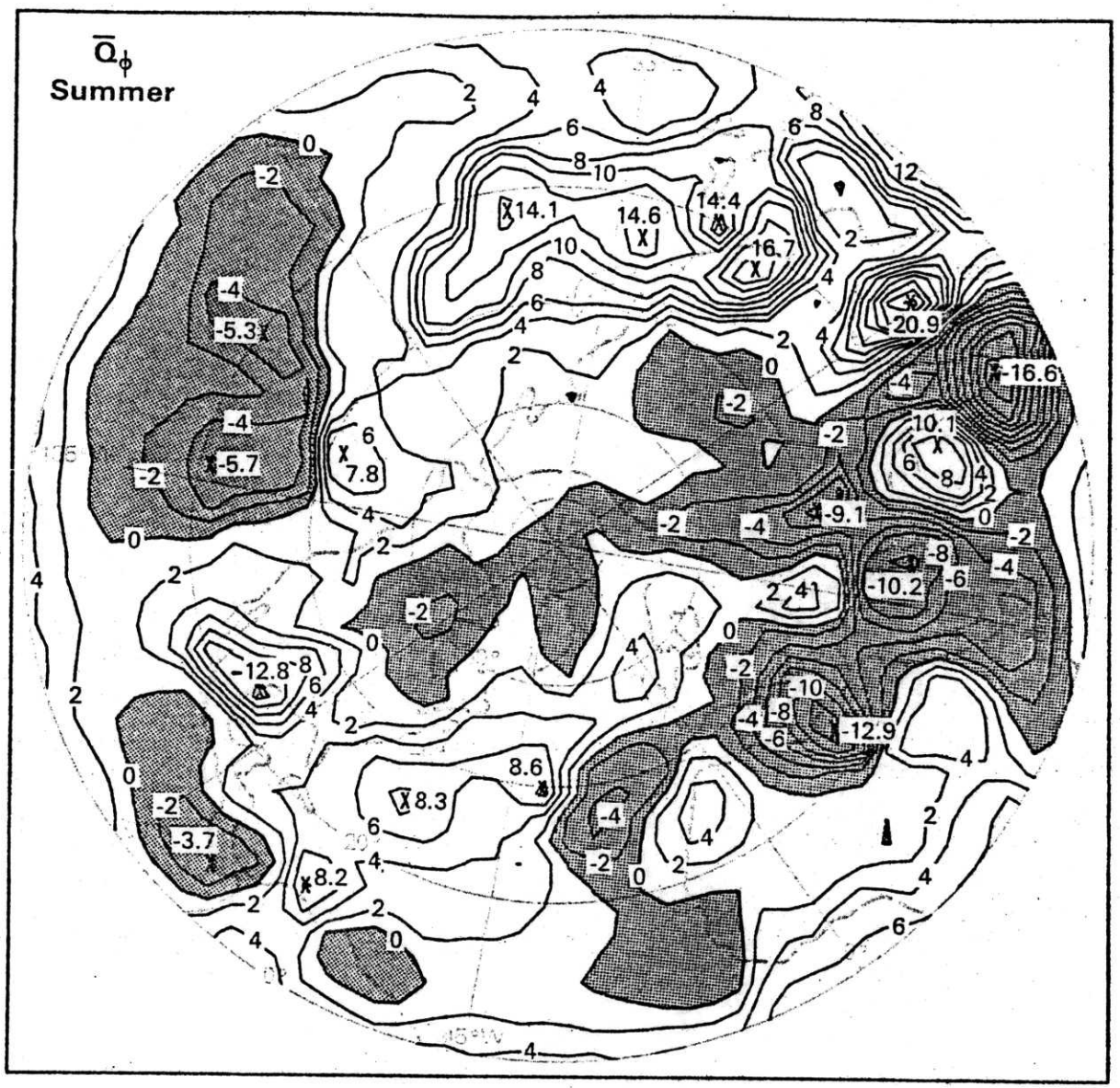

Figure 8. Hemispheric distribution of the vertically integrated meridional moisture transport, Q_ϕ, for composite summer season during 1 May 1958 - 30 April 1963 (from Peixoto et al., 1980). Units are 10 kg $s^{-1}m^{-1}$. Negative values indicate westward flow.

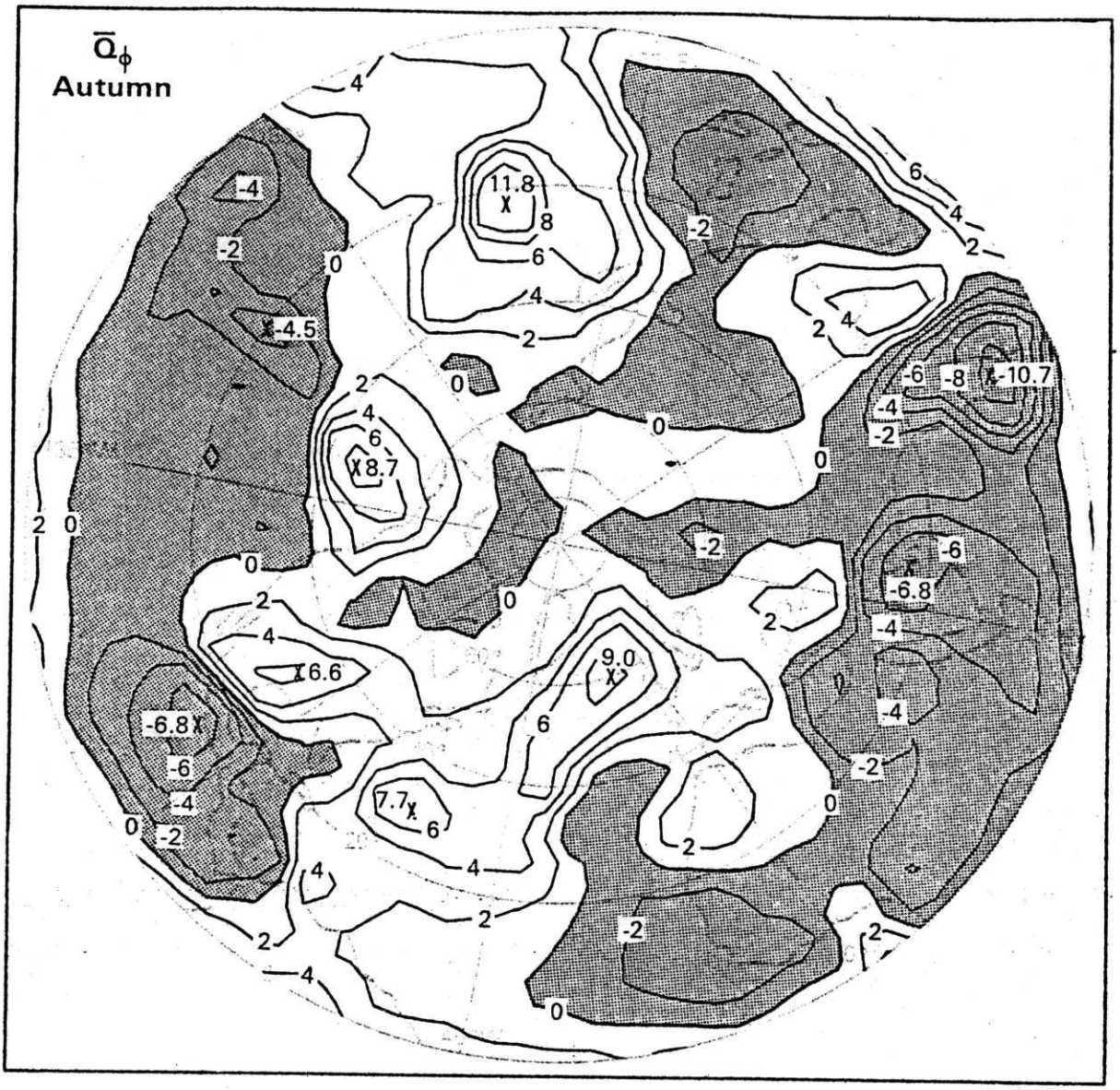

Figure 9. Hemispheric distribution of the vertically integrated meridional moisture transport, Q_ϕ, for composite autumn season during 1 May 1958 - 30 April 1963 (from Peixoto et al., 1980). Units are 10 kg s^{-1} m^{-1}. Negative values indicate westward flow.

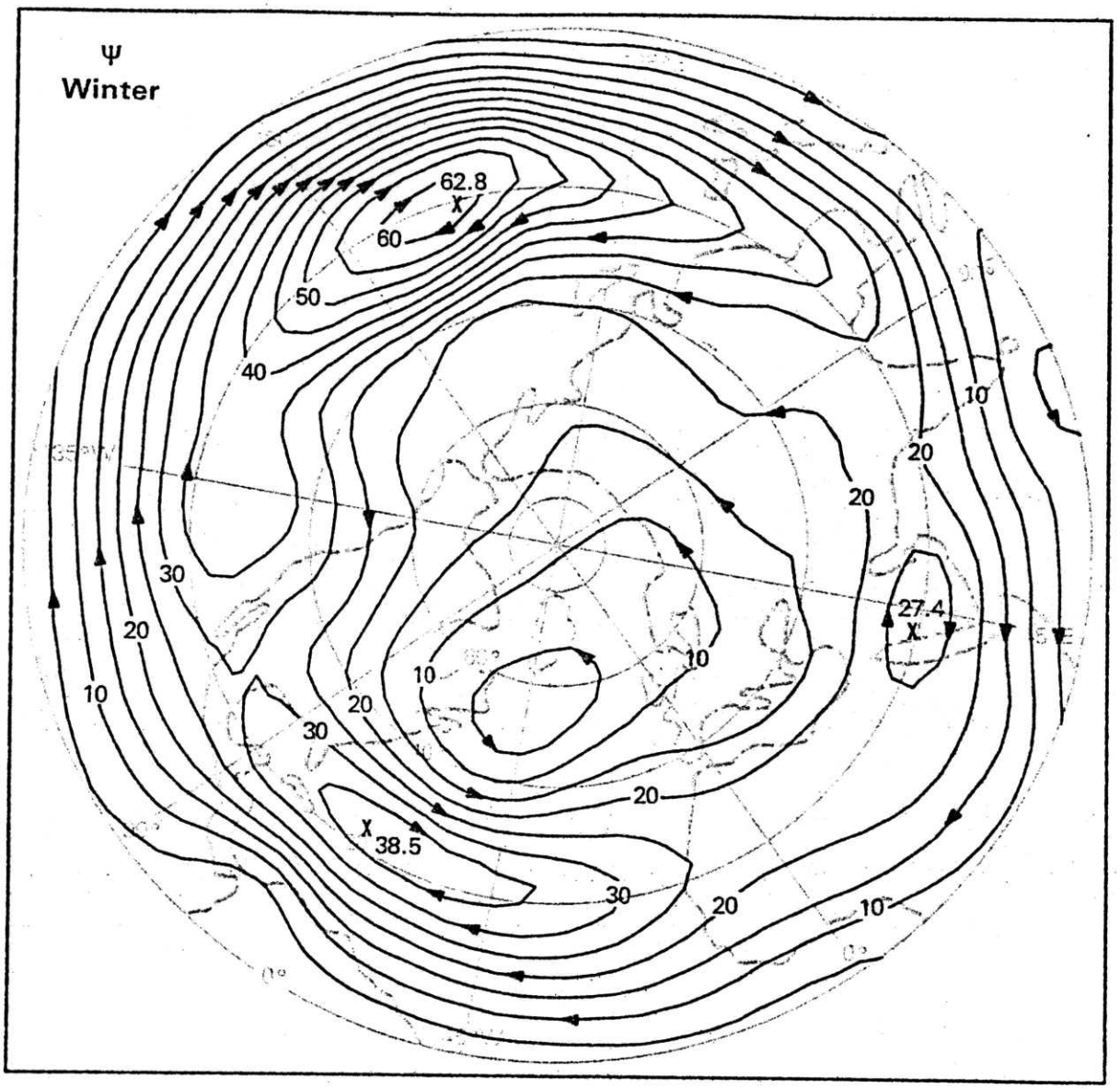

Figure 10. Hemispheric distribution of the streamfunction for the vertically integrated moisture transport, ψ , for composite winter season during 1 May 1958 - 30 April 1963 (from Peixoto et al., 1980). Units are 10^7kg s^{-1} and arrows indicate the sense of circulation.

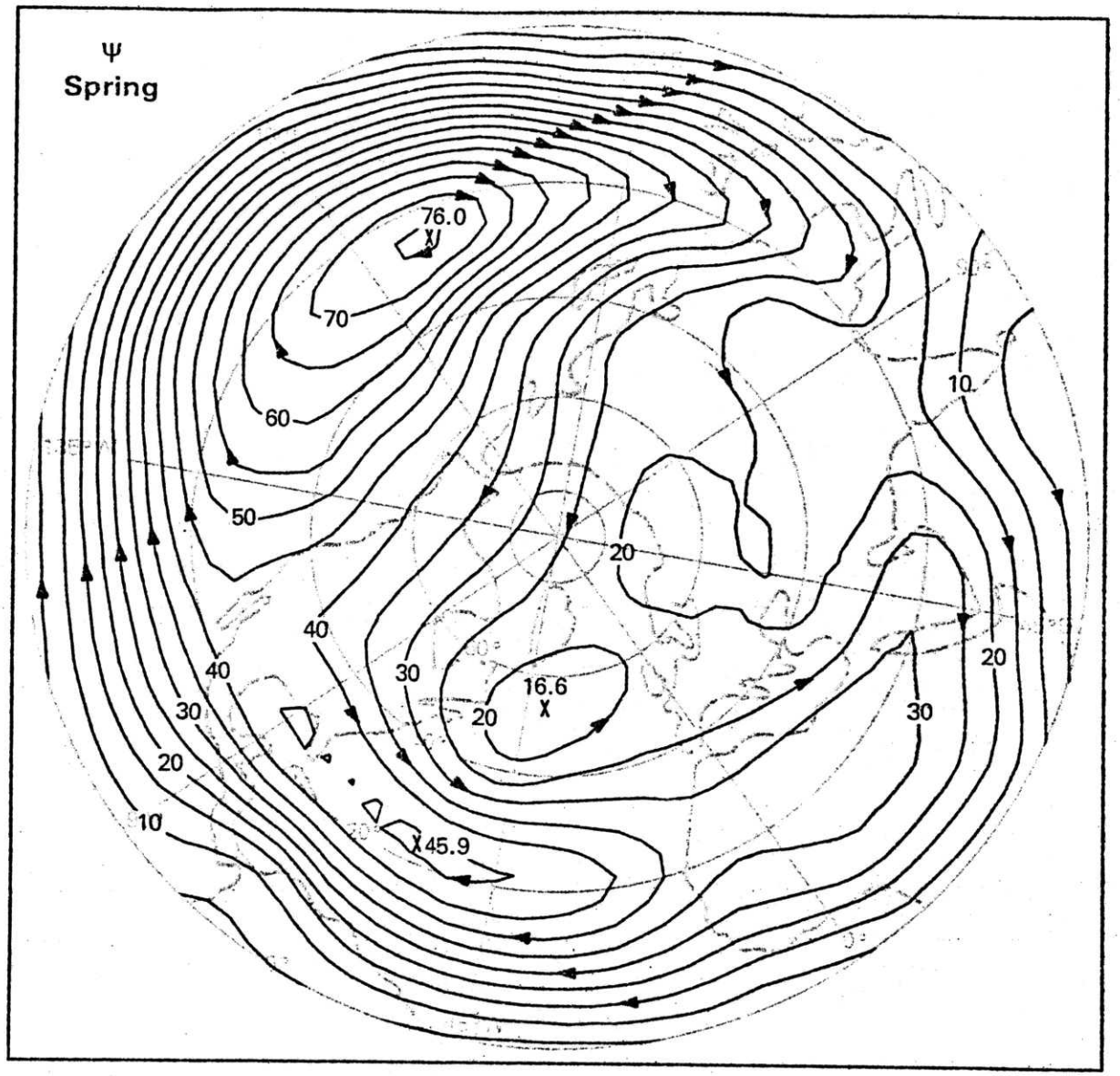

Figure 11. Hemispheric distribution of the streamfunction for the vertically integrated moisture transport, ψ, for composite spring season during 1 May 1958 - 30 April 1963 (from Peixoto et al., 1980). Units are 10^7 kg s^{-1} and arrows indicate the sense of circulation.

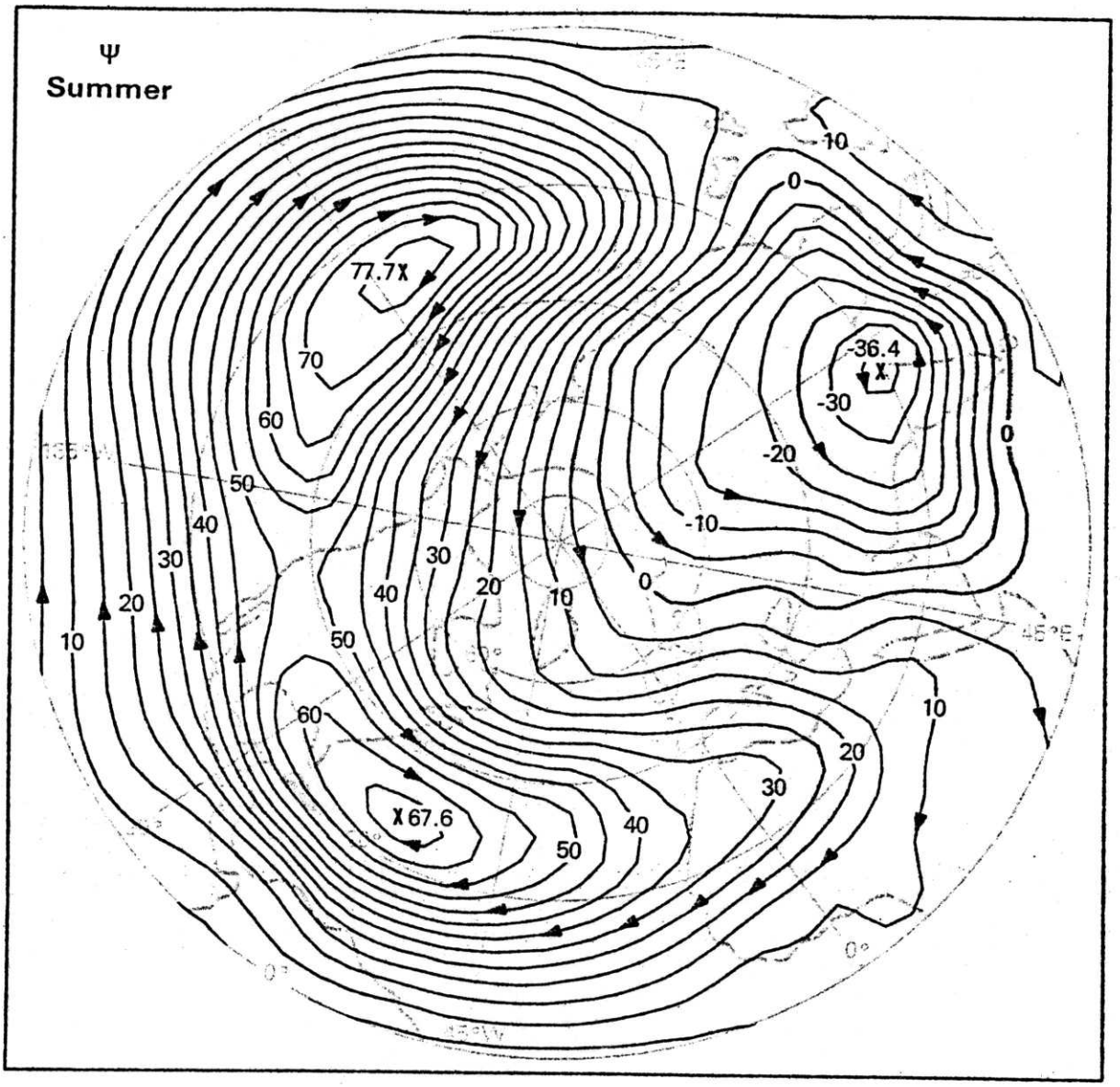

Figure 12. Hemispheric distribution of the streamfunction for the vertically integrated moisture transport, ψ, for composite summer season during 1 May 1958 - 30 April 1963 (from Peixoto et al., 1980). Units are $10^7 kg\ s^{-1}$ and arrows indicate the sense of circulation.

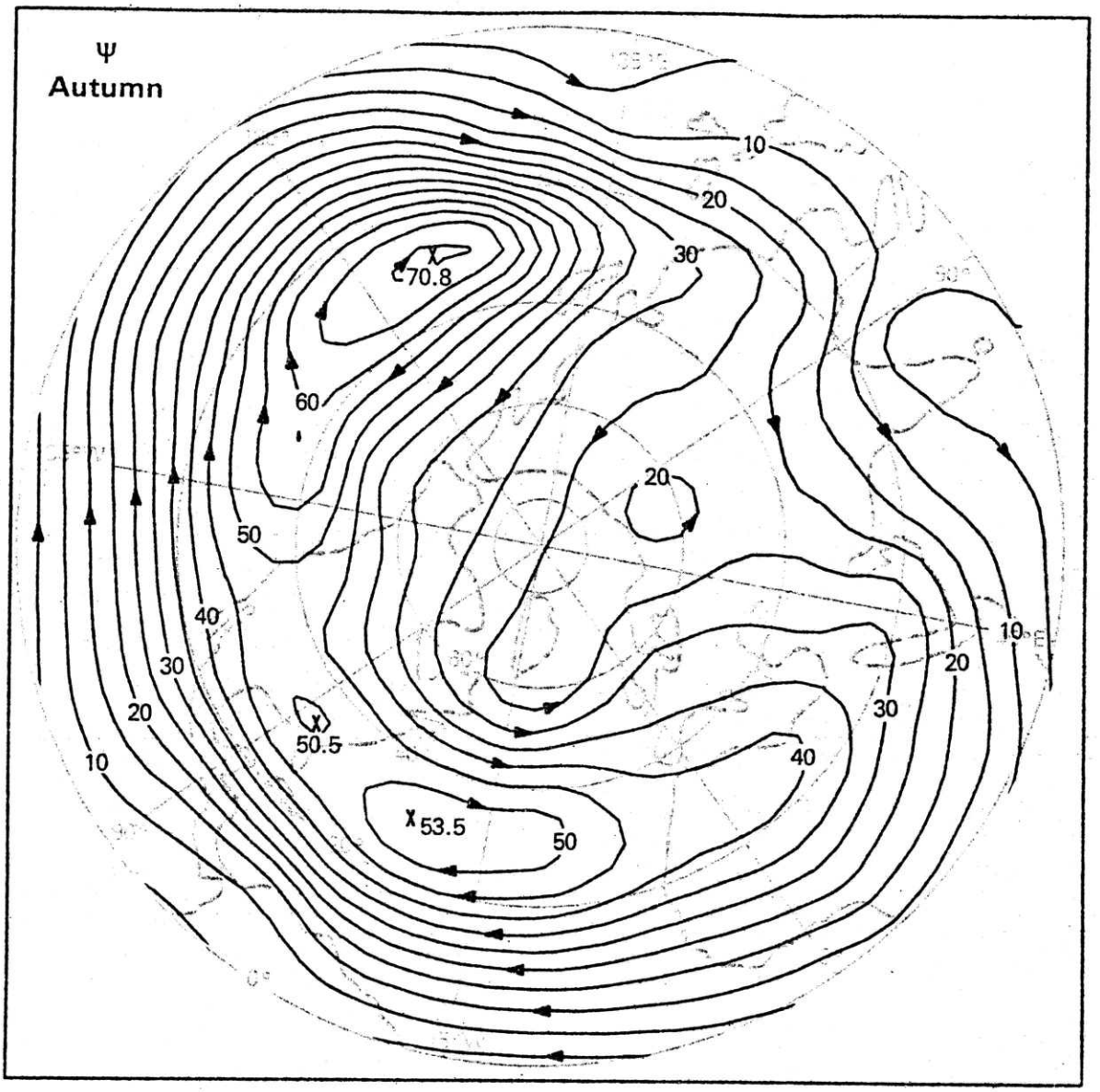

Figure 13. Hemispheric distribution of the streamfunction for the vertically integrated moisture transport, ψ, for composite autumn season during 1 May 1958 - 30 April 1963 (from Peixoto et al., 1980). Units are $10^7 kg\ s^{-1}$ and arrows indicate the sense of circulation.

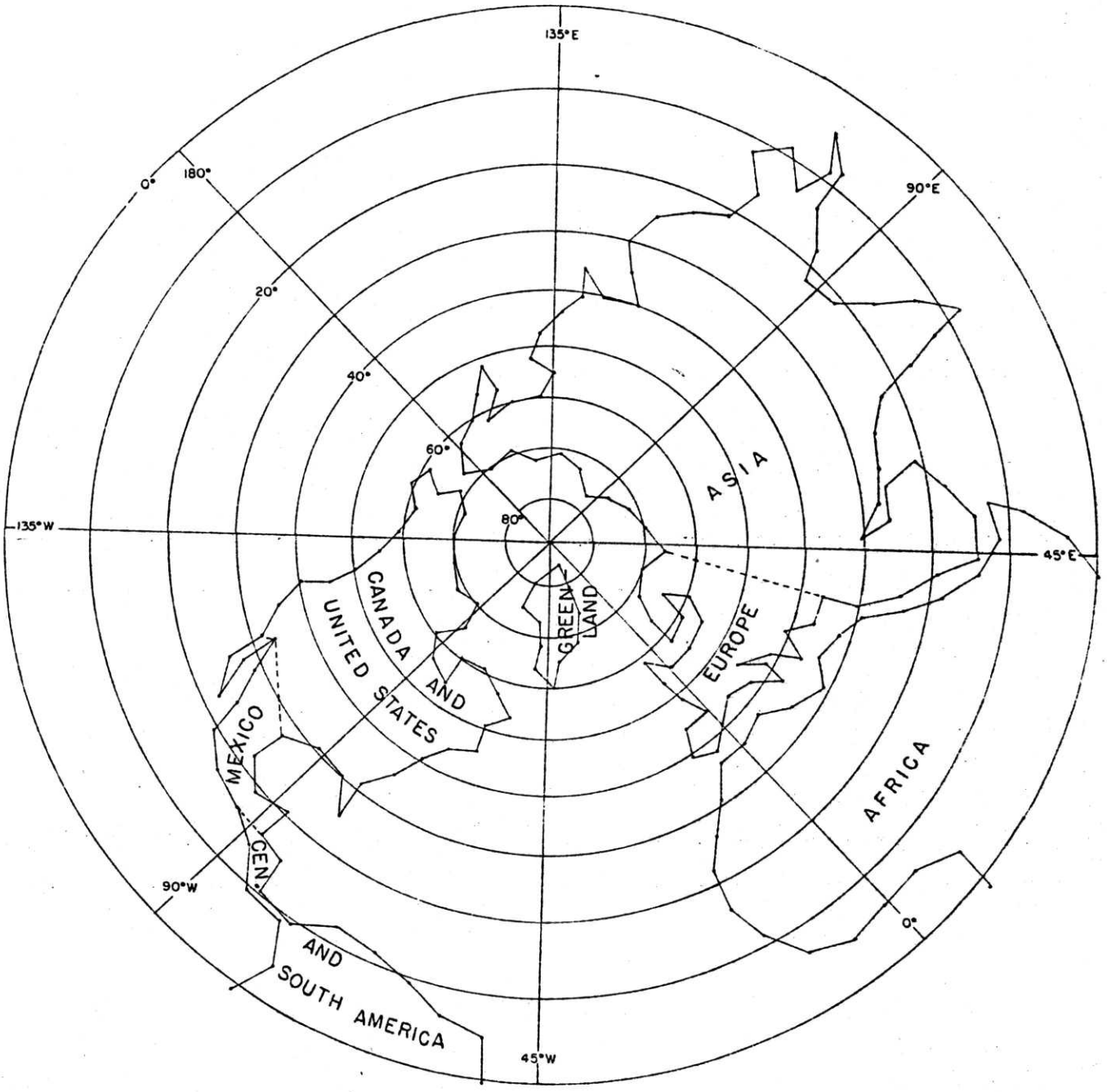

Figure 14. Base map of the continents as reconstructed for this study.

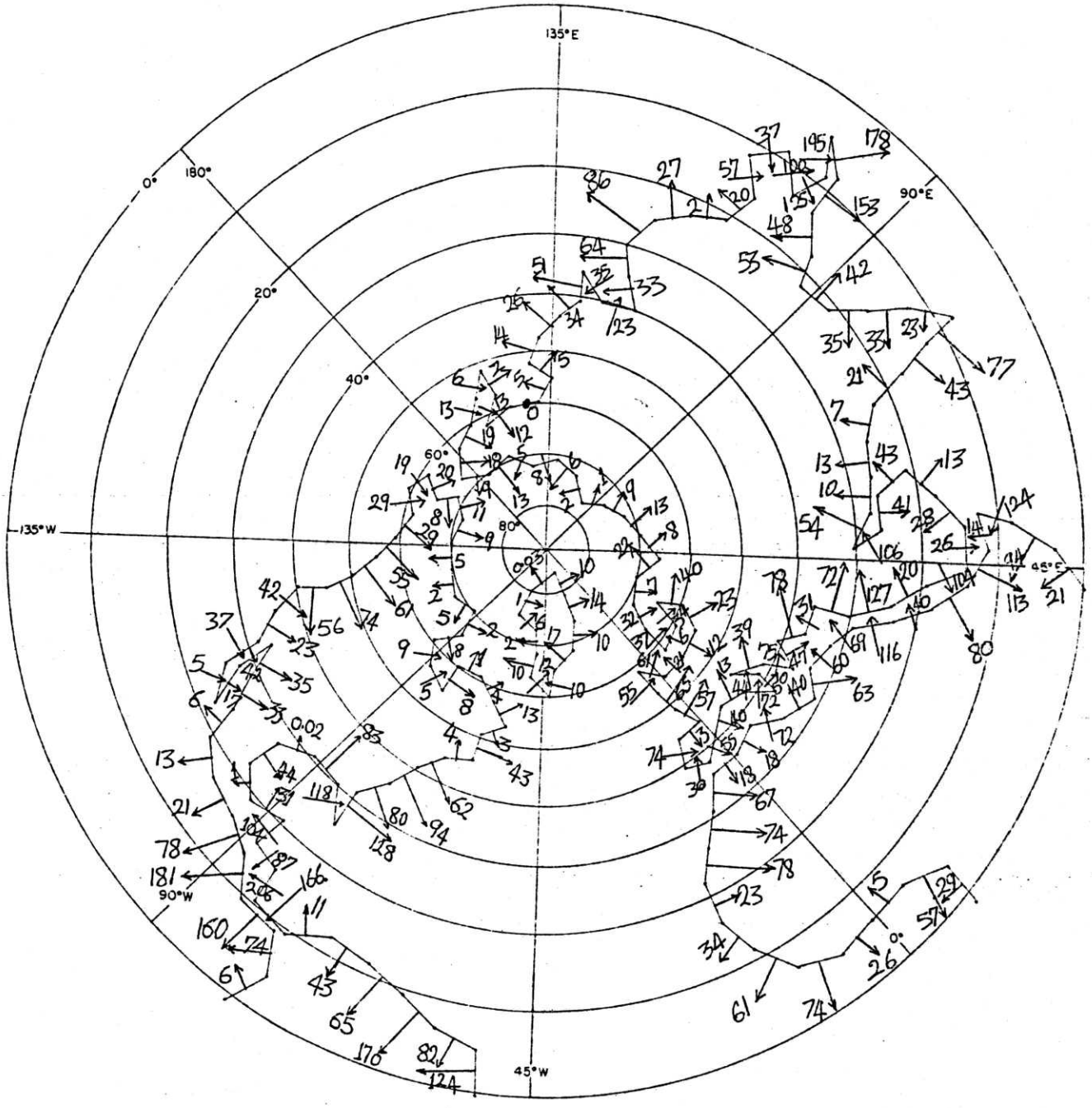

Figure 15. Landward moisture fluxes in winter. Units are in $kg.s^{-1}m^{-1}$.

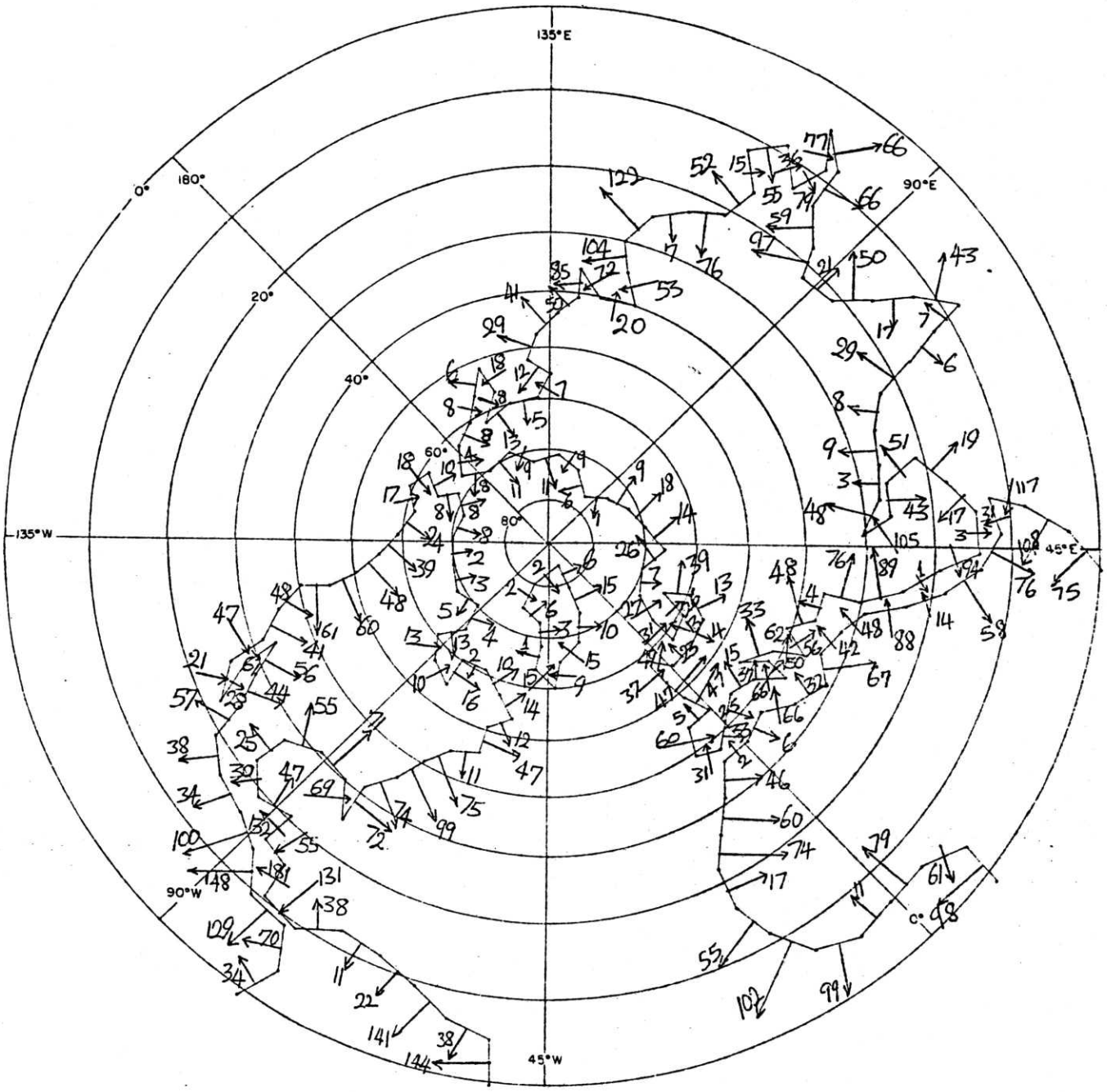

Figure 16. Landward moisture fluxes in s.pring. Units are in $kg\,s^{-1}\,m^{-1}$.

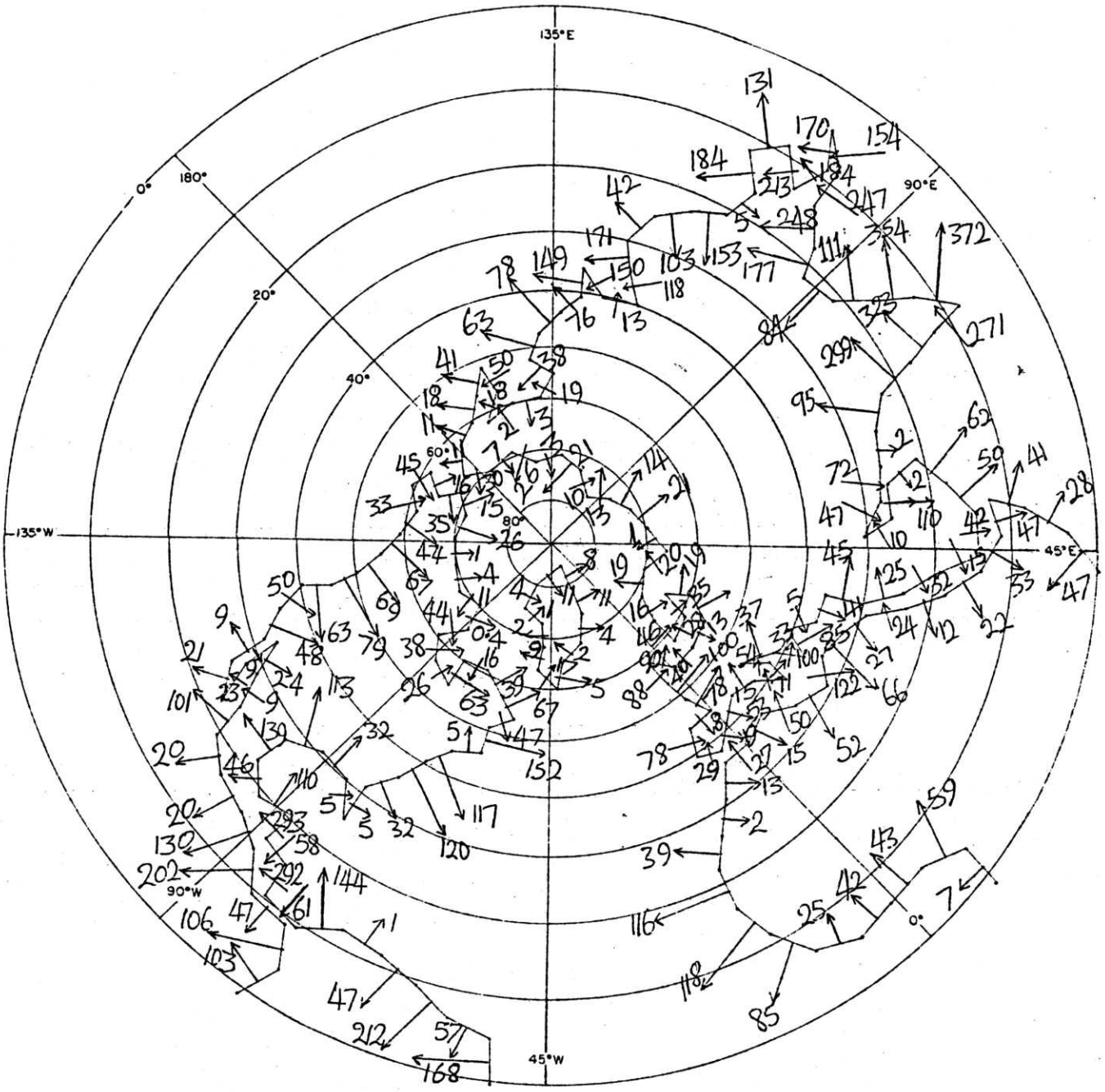

Figure 17. Landward moisture fluxes in summer. Units are in kg s^{-1} m^{-1}.

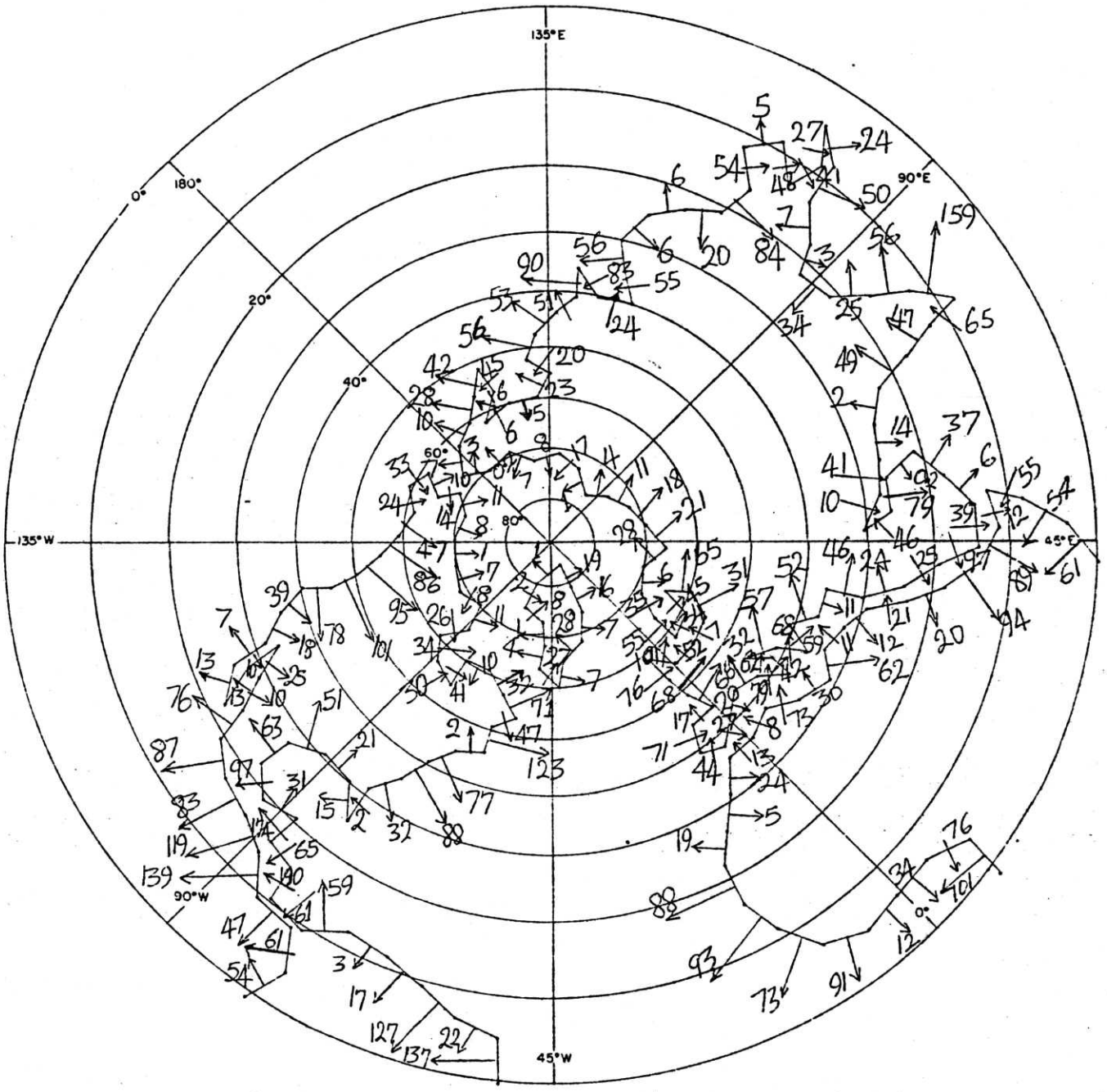

Figure 18. Landward moisture fluxes in autumn. Units are in $kg\,s^{-1}\,m^{-1}$.

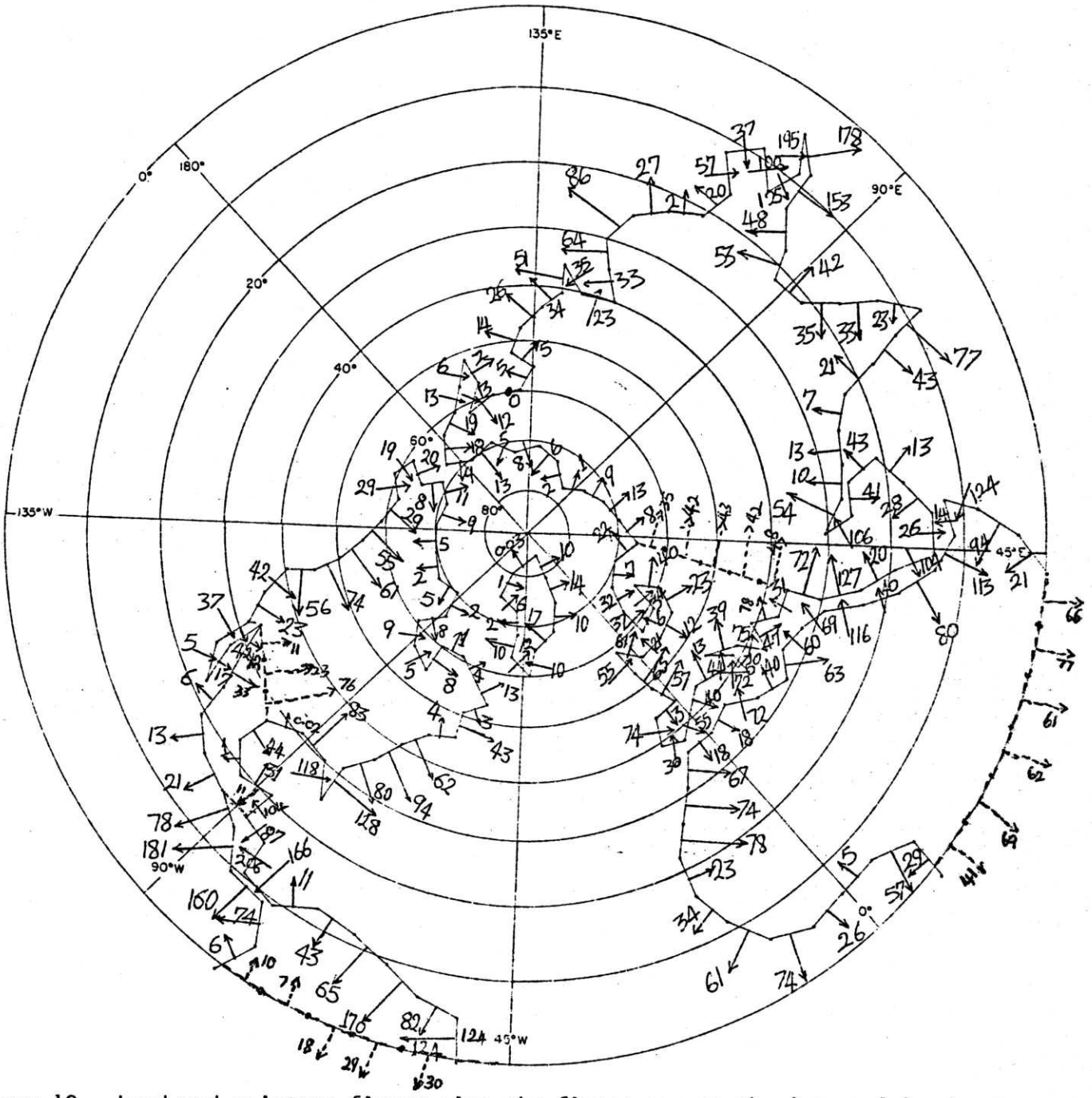

Figure 19. Landward moisture fluxes plus the fluxes across the internal borders in winter. Units are kg $s^{-1}m^{-1}$.

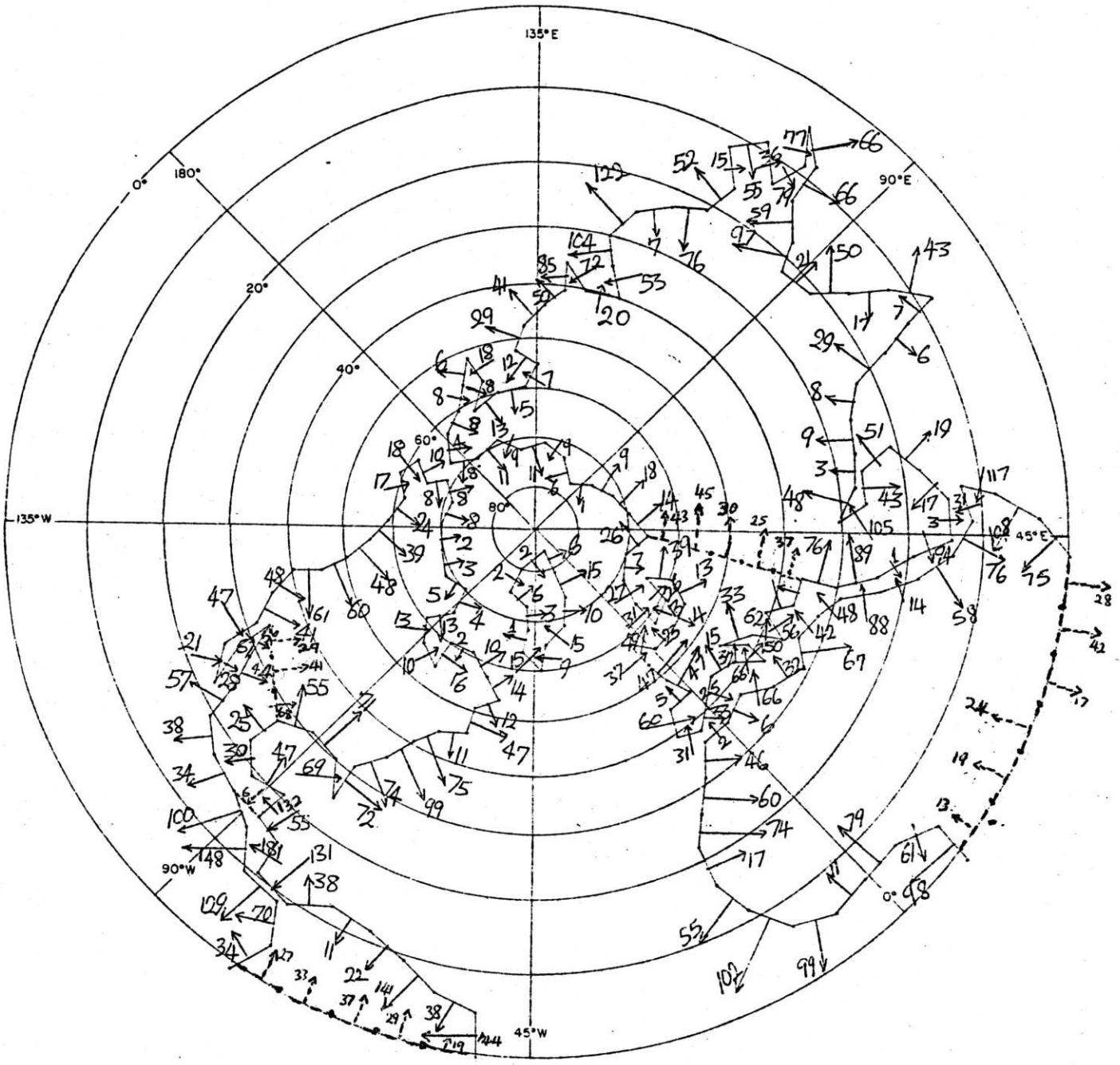

Figure 20. Landward moisture fluxes plus the fluxes across the internal borders in spring. Units are kg $s^{-1}m^{-1}$.

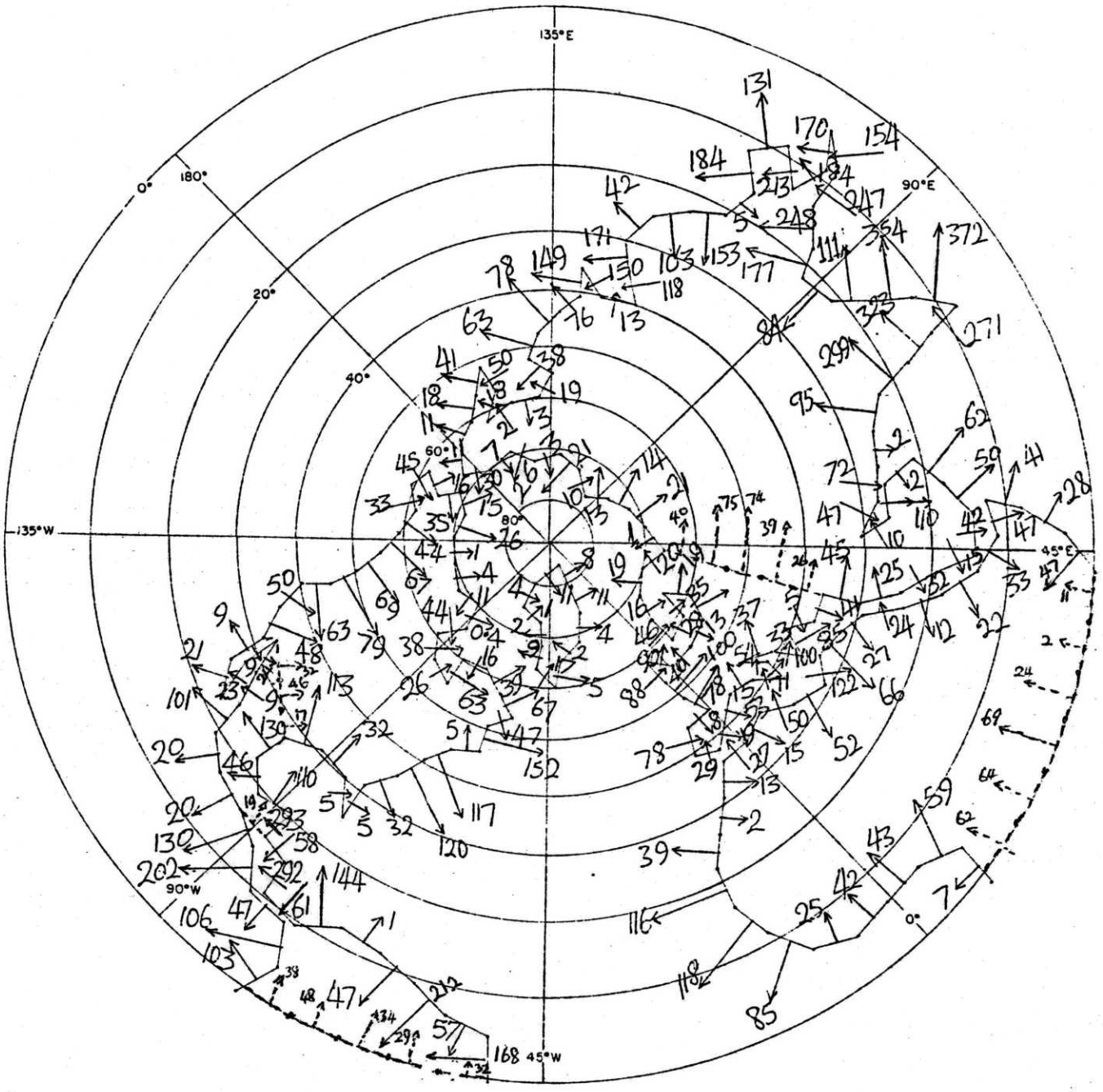

Figure 21. Landward moisture fluxes plus the fluxes across the internal borders in summer. Units are kg $s^{-1}m^{-1}$.

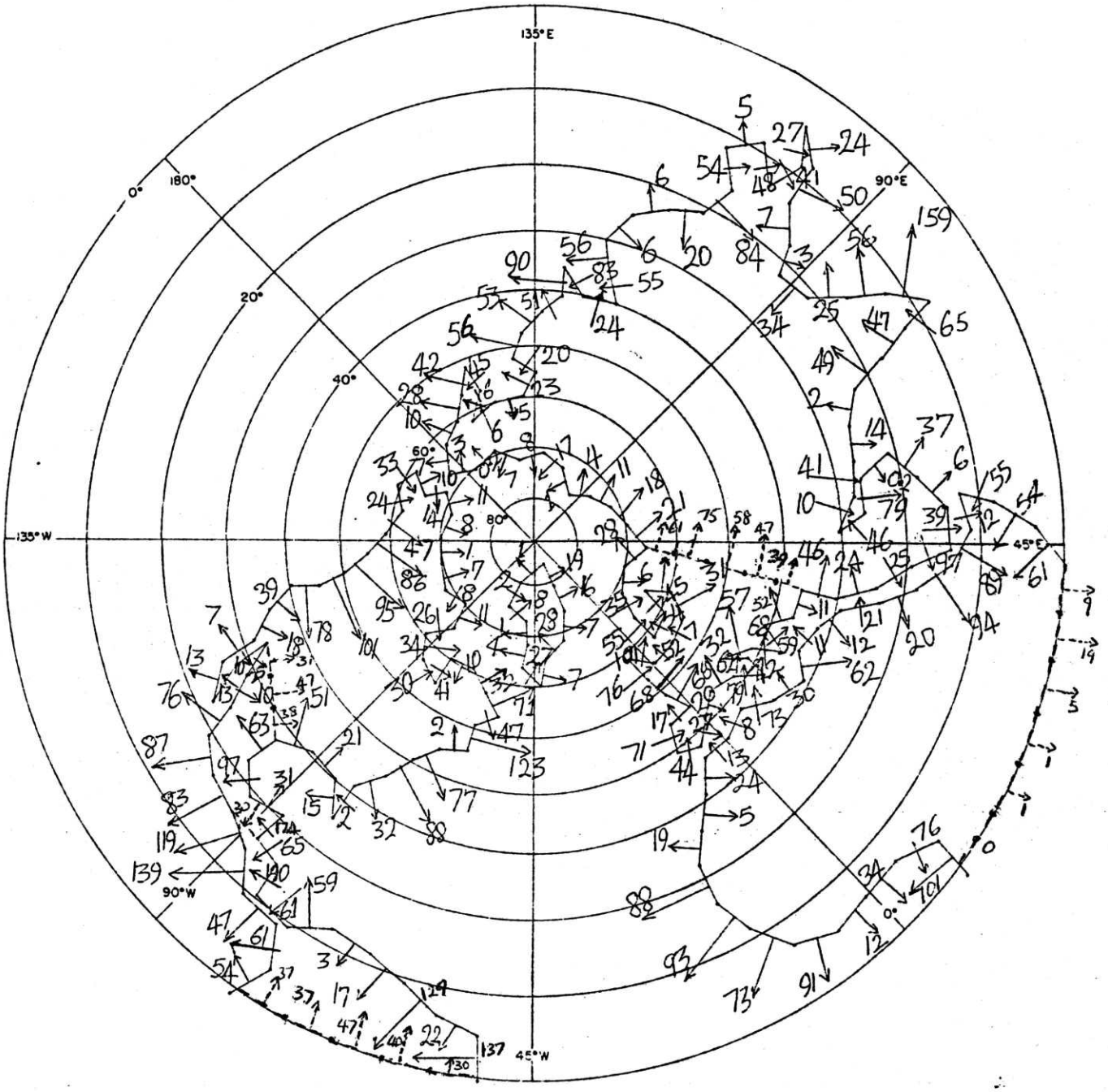

Figure 22. Landward moisture fluxes plus the fluxes across the internal borders in autumn. Units are kg $s^{-1}m^{-1}$.

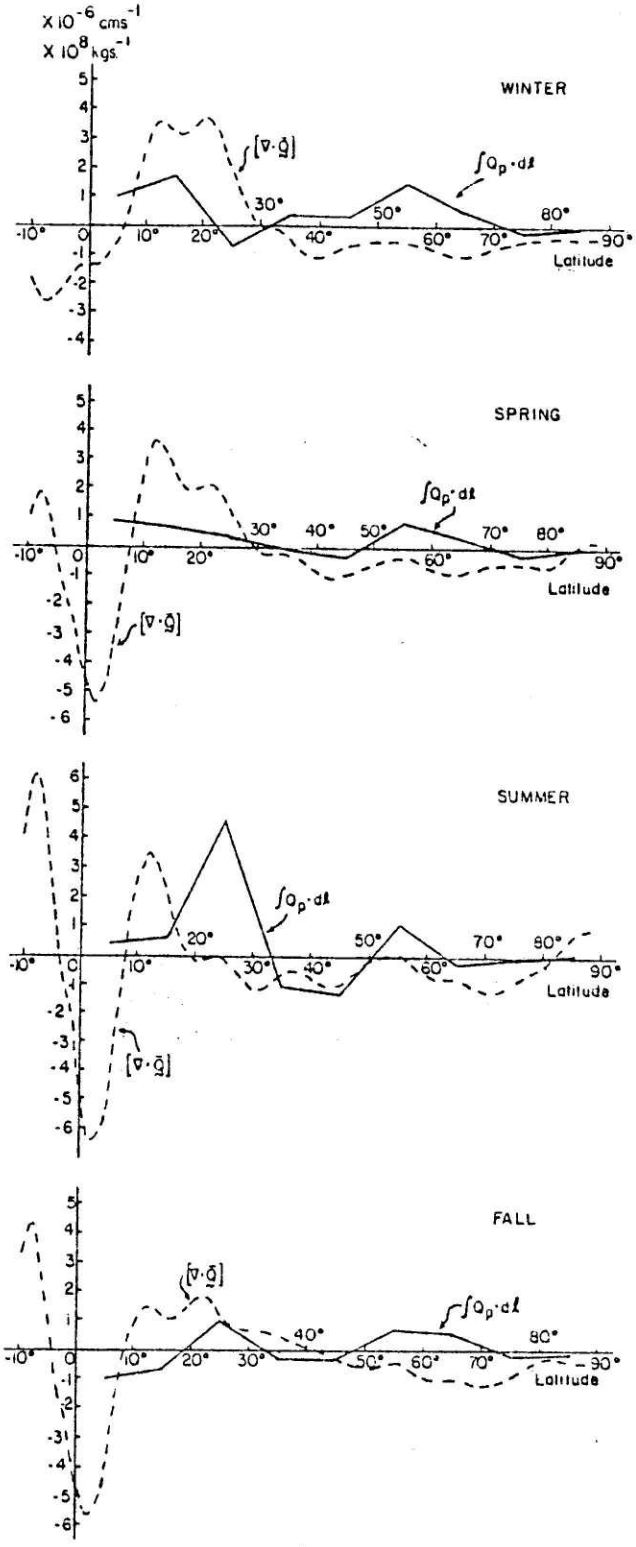

Figure 23. Plot of the landward moisture transports as a function of latitude and the zonally averaged water vapor divergence for the complete latitude belt. Units for the former are 10^8kg s^{-1} and for the latter 10^{-6}cm s^{-1}.

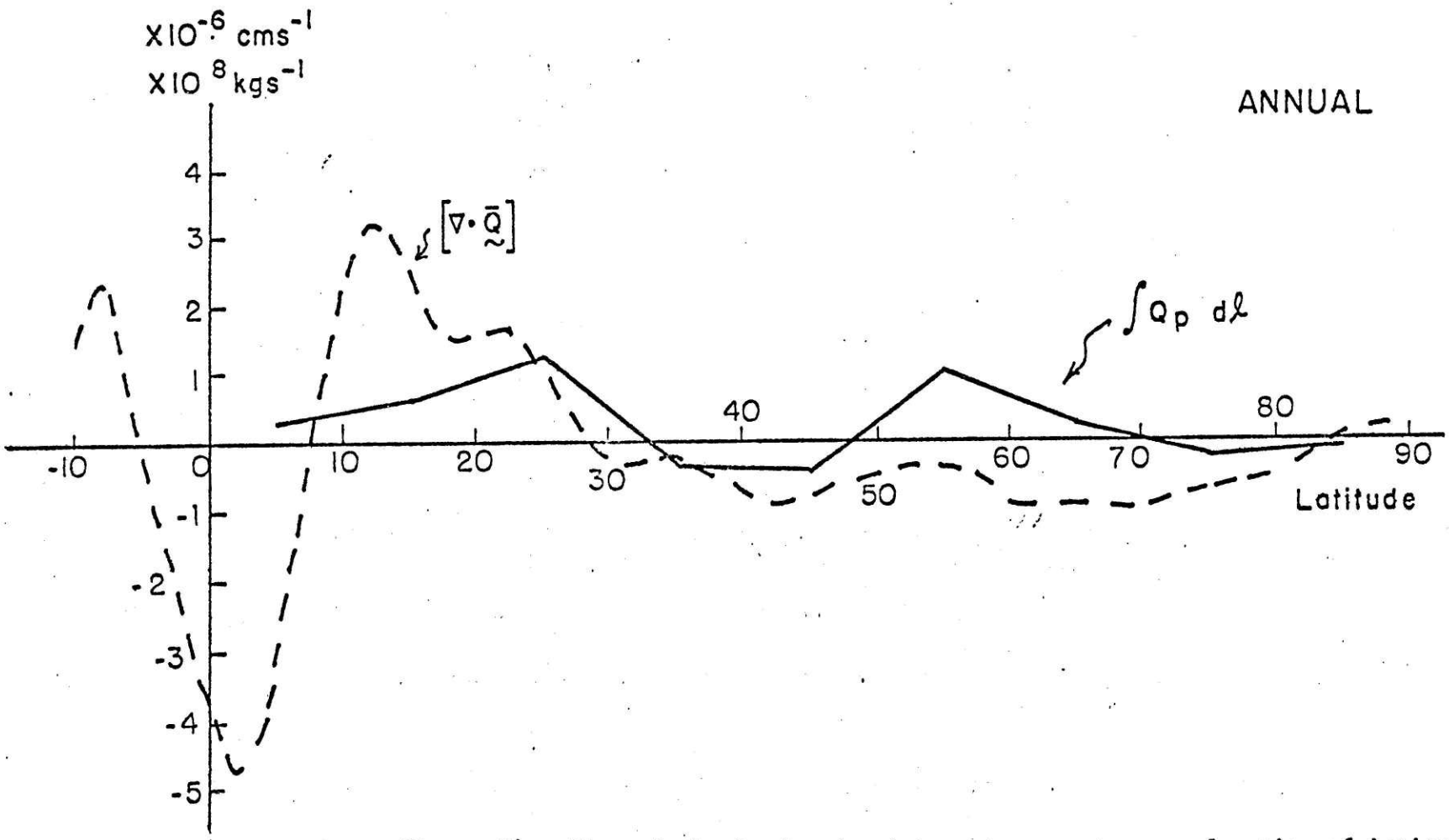

Figure 24. Plot of the landward moisture transports as a function of latitude and the zonally averaged water vapor divergence for the complete latitude belt. Units for the former are 10^8kg s^{-1} and for the latter 10^{-6}cm s^{-1}.

LIST OF TABLES

Table Number		Page
I	The number of coastal segments, length of the coast and the area for each of the regions shown on the base map in Figure 14.	68
II	Integral of the water vapor transports normal to the borders, along the entire borders of each of the regions studied, during all seasons. Units are 10^8kg s^{-1}.	69
III	Excess of precipitation over evapotranspiration for all the regions studied, during all seasons. Units are cm $(3mo)^{-1}$.	70
IV	Integral of the water vapor transports, normal to the coast, along the coasts only, for each of the regions studied during all seasons. Units are 10^8kg s^{-1}.	71
V	Integral of the landward water vapor transports within 10° latitude belts during all seasons. Units are 10^8kg s^{-1}.	72
VI	Summary results relating zonally averaged moisture divergence to the landward flux within latitude bands.	73

Table 1. The number of coastal and internal border segments, length of of the coast and the area for each of the regions shown in Figure 14. 1 segment = 300 nautical miles = 555.6 km.

	Number of segments		Length of coasts (10^4km)	Area (10^6km^2)
	Coastal	Internal borders		
CONTINENTS				
America	61	5	3.39	22.47
Africa	26	6	1.44	20.31
Greenland	11	0	0.61	1.92
Europe	28	5	1.56	7.57
Asia	62	5	3.45	41.93
Northern Hemisphere	188	11	10.45	94.19
SUBCONTINENTS				
United States and Canada	34	3	1.89	17.16
Mexico	13	4	0.72	1.89
Central and South America	14	6	0.78	3.42

Table II. Integral of the water vapor transports normal to the borders along the entire borders of each of the regions studied, during all seasons. Units are 10^8 kg s^{-1}.

Season\Continents	America	Africa	Greenland	Europe	Asia	Northern Hemisphere
Winter	3.05	-1.62	0.00	0.93	-0.29	2.07
Spring	2.95	0.15	0.10	0.41	-0.27	3.34
Summer	3.29	1.71	-0.02	-0.45	1.75	6.34
Autumn	2.53	-1.62	-0.05	0.50	-0.96	0.51
Annual	2.96	-0.35	0.01	0.35	0.06	3.07

Season\Subcontinents	US plus Canada	Mexico	Central and South America
Winter	1.31	-0.44	2.19
Spring	1.29	-0.31	1.96
Summer	0.67	0.84	1.79
Autumn	0.90	-0.40	2.04
Annual	1.04	-0.08	2.00

Table III. Excess of precipitation over evapotranspiration for all the regions studied, during all seasons. Units are cm(3mo.)$^{-1}$.

Season \ Continents	America	Africa	Greenland	Europe	Asia	Northern Hemisphere
Winter	10.6	-6.2	0.1	9.6	-0.5	1.7
Spring	10.2	0.58	4.0	4.2	-0.5	2.8
Summer	11.4	6.6	-0.9	-4.6	3.2	5.2
Autumn	8.8	-6.2	2.2	5.1	-1.8	0.4
Annual	10.3	-1.3	1.4	3.5	0.1	2.5

Season \ Subcontinents	US plus Canada	Mexico	Central and South America
Winter	5.9	-18.3	49.7
Spring	5.9	-12.7	44.6
Summer	3.1	34.4	40.6
AUtumn	4.1	-16.5	46.3
Annual	4.8	-3.3	45.3

Table IV Integral of the vertically integrated water vapor transports normal to the coast (coast only), for each of the regions studied, during all seasons. Negative signs depict net oceanward transports. Units are 10^8kg s^{-1}.

Season\Continents	America	Africa	Greenland	Europe	Asia	Northern Hemisphere
Winter	3.38	0.47	0.00	2.09	-1.46	4.49
Spring	2.14	0.32	0.10	1.40	-1.26	2.70
Summer	2.29	0.44	-0.02	0.95	0.34	4.00
Autumn	1.47	-1.43	0.05	2.05	-2.51	-0.36
Annual	2.32	-0.05	0.03	1.62	-1.22	2.71

Season\Subcontinents	US plus Canada	Mexico	Central and South America
Winter	0.70	0.23	2.46
Spring	0.53	0.49	1.13
Summer	0.14	1.26	0.89
Autumn	0.25	0.41	0.81
Annual	0.41	0.60	1.32

Table V. Integral of the landward water vapor transports within 10° latitude belts during all seasons. Negative signs depict net oceanward transports. Units are 10^8 kg s^{-1}.

Latitude band \ Season	Winter	Spring	Summer	Autumn	Annual	N
0-10	1.03	0.91	0.42	-1.01	0.34	20
11-20	1.71	0.74	0.56	-0.71	0.58	31
21-30	-0.72	0.38	4.55	1.02	1.31	30
31-40	0.41	-0.13	-1.00	-0.32	-0.26	27
41-50	0.32	-0.25	-1.29	-0.30	-0.38	15
51-60	1.45	0.87	1.13	0.67	1.03	27
61-70	0.51	0.43	-0.25	0.59	0.32	25
71-80	-0.16	-0.23	-0.14	-0.18	-0.18	11
81-90	-0.05	-0.03	0.02	-0.11	-0.04	2

N = Number of transport values (or segment midpoints) that went into computing the net transport for that latitude band.

Table VI. Summary results relating zonally averaged moisture divergence to the landward flux within latitude bands.

Latitude bands (°N)	$[\nabla \cdot \bar{Q}]$ (land and ocean)	$\int Q_p \, dl$ (along coasts only)
0-10°	P > E	landward
10-30	E > P	landward
30-50	P > E	oceanward
50-70	P > E	landward
above 70	P > E	oceanward